Design, Synthesis, and Biological Investigation of New Binaphthalene Precursors as Efficient Photo-Activated DNA Interstrand Cross-Linkers

Supporting Information

Contents:

1. UV absorption spectra for different compounds (200 μM).
2. Solvent dependent DNA ICL formation.
3. pH dependent DNA ICL formation.
4. Time dependent DNA ICL formation.
5. Concentration dependent DNA ICL formation.
6. $MeONH_2$ and TEMPO trapping assay.
7. Determination of DNA alkylation sites.
8. NMR spectra.
9. Mass spectra of new compounds.

1. UV absorption spectra for different compounds (200μM)

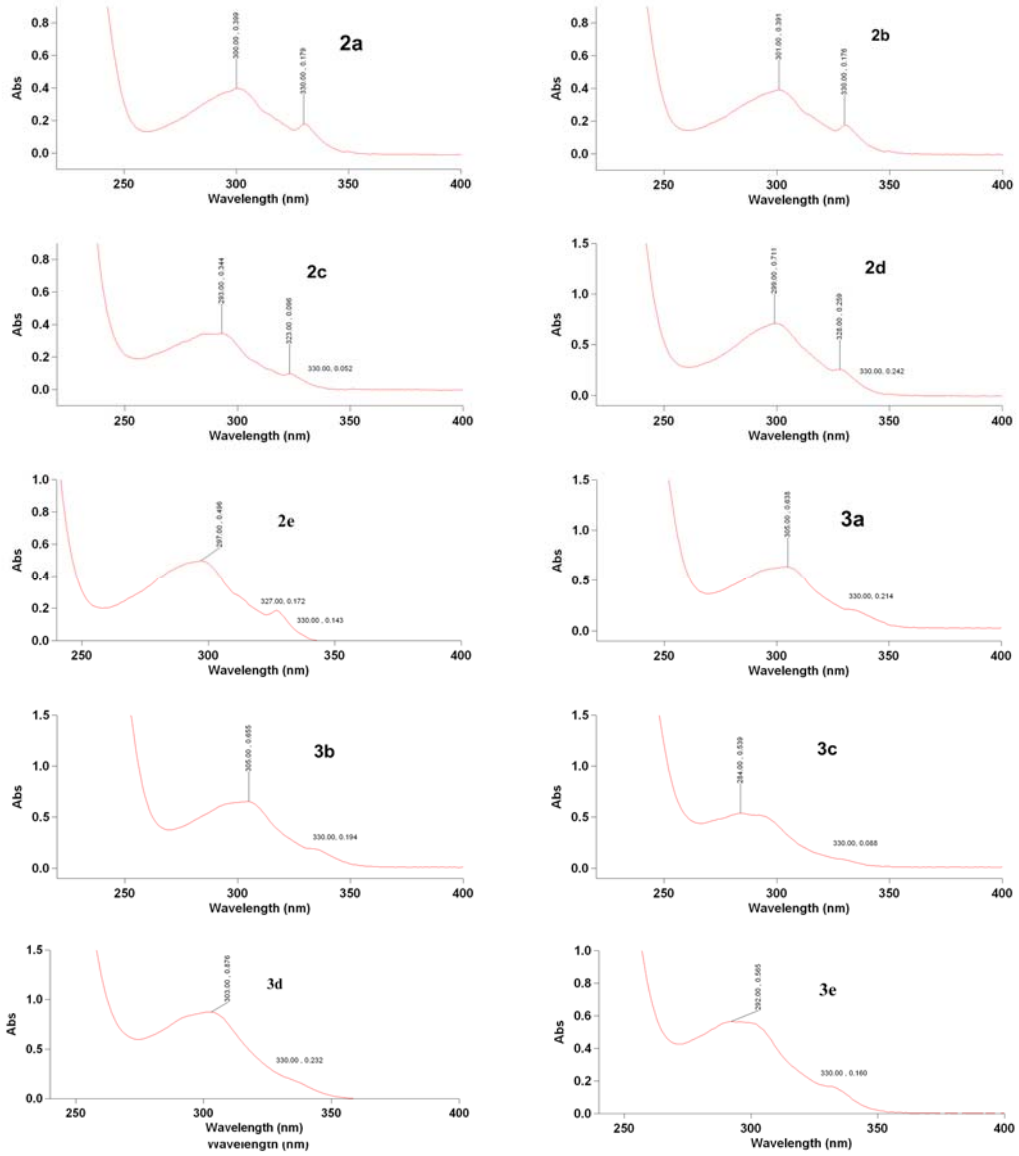

Figure S1. UV absorption spectra for **2a-e** in $CHCl_3$ and **3a-e** in MeOH with 0.2 mM concentration.

2. Solvent dependent DNA ICL formation.

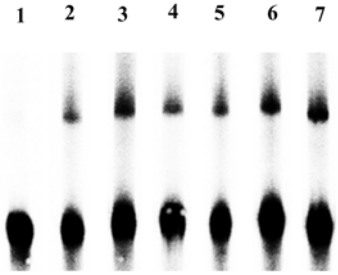

Figure S2. Representative gel of solvent dependence for DNA cross-link formation induced by **3b** (500 μM) upon UV irradiation. Lane 1: with DNA only; Lane 2: H_2O (cross-linking yield 19.8%); lane 3: H_2O/CH_3CN (7:3) (30.3%); lane 4: H_2O/MeOH (7:3) (20.7%); lane 5: H_2O/DMF (7:3) (26.0%); lane 6: H_2O/DMSO (7:3) (23.9%); lane 7: H_2O/THF (7:3) (22.2%). Condition: duplex **13** was irradiated by 350 nm light for 6h.

3. pH dependent DNA ICL formation.

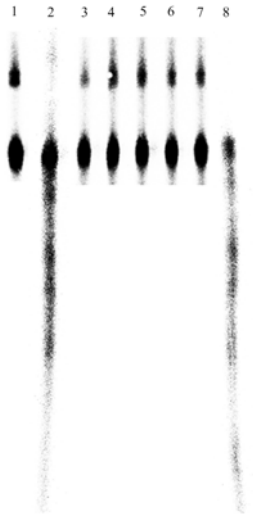

Figure S3. Representative gel of pH dependence for DNA cross-link formation induced by **3b** (500 μM) upon UV irradiation. Lane 1: pure H_2O (cross-linking yield 31.9%); Lane 2: pH 4.47 KH_2PO_3 buffer (not determined); lane 3: pH 5.00 K_2HPO_3/KH_2PO_3 buffer (30.9%); lane 4: pH 6.00 K_2HPO_3/KH_2PO_3 buffer (37.8%); lane 5: pH 7.00 K_2HPO_3/KH_2PO_3 buffer (38.7%); lane 6: pH 8.00 K_2HPO_3/KH_2PO_3 buffer (36.8%); lane 7: pH 8.68 K_2HPO_3 buffer (34.5%); lane 8: pH 12.58 K_3PO_3 buffer (not determined). Condition: duplex **13** was irradiated by 350 nm light for 8 h.

4. Time dependent DNA ICL formation

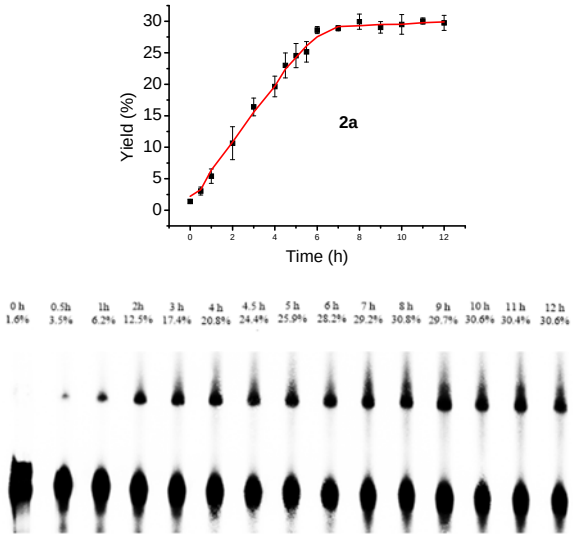

Figure S4. The time dependence of DNA ICL formation of duplex **13** for **2a** (500 μM) upon 350 nm irradiation.

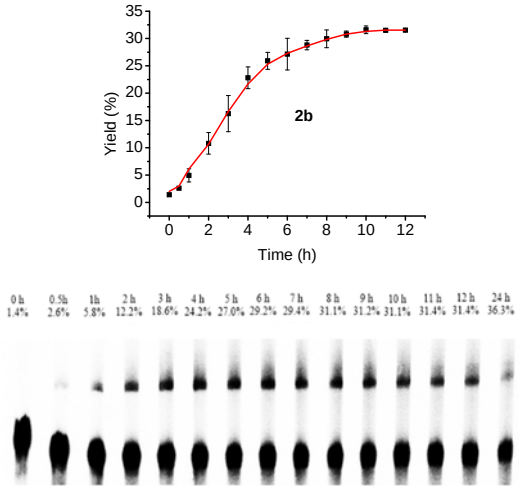

Figure S5. The time dependence of DNA ICL formation of duplex **13** for **2b** (500 μM) upon 350 nm irradiation.

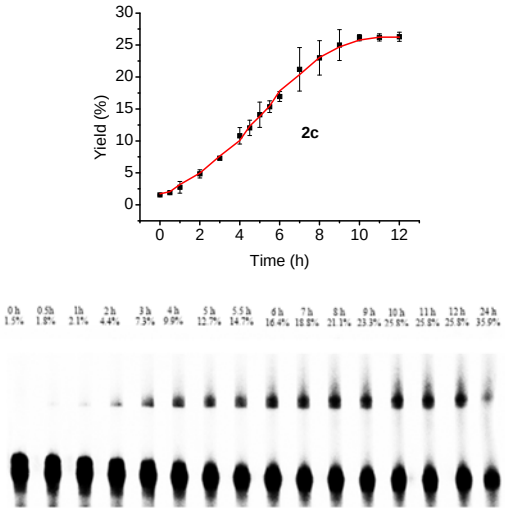

Figure S6. The time dependence of DNA ICL formation of duplex **13** for **2c** (500 μM) upon 350 nm irradiation.

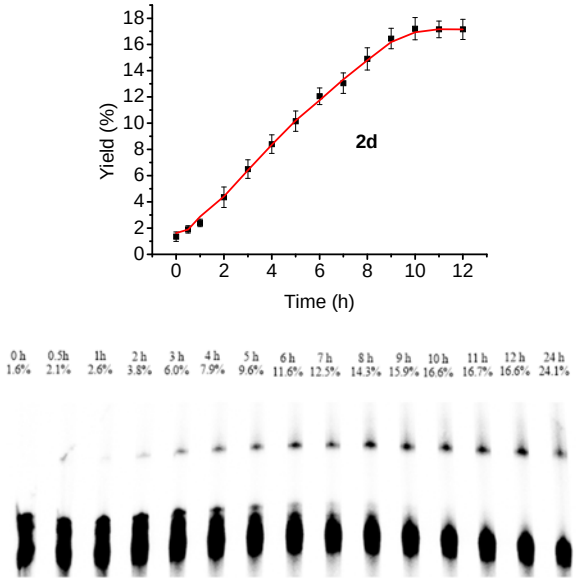

Figure S7. The time dependence of DNA ICL formation of duplex **13** for **2d** (500 μM) upon 350 nm irradiation.

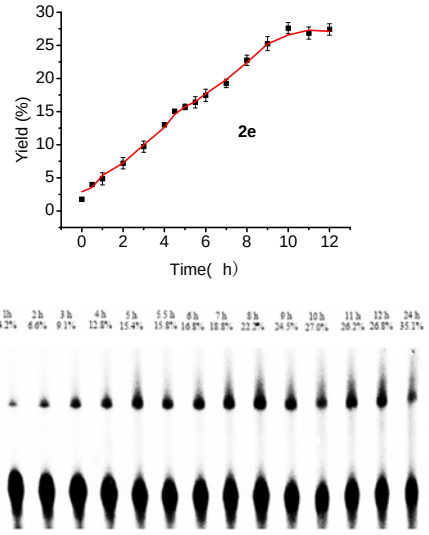

Figure S8. The time dependence of DNA ICL formation of duplex **13** for **2e** (500 μM) upon 350 nm irradiation.

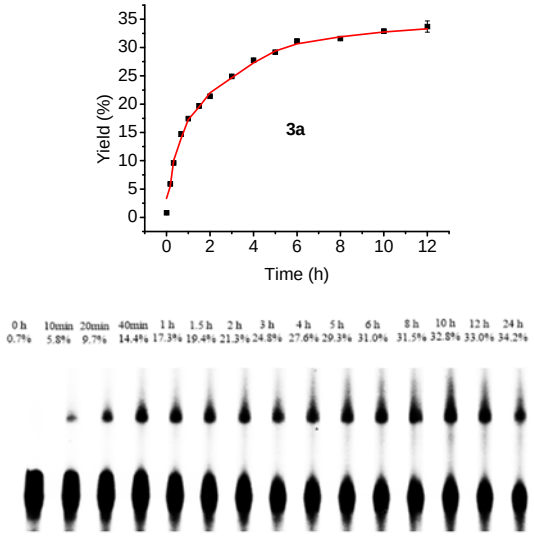

Figure S9. The time dependence of DNA ICL formation of duplex **13** for **3a** (500 μM) upon 350 nm irradiation.

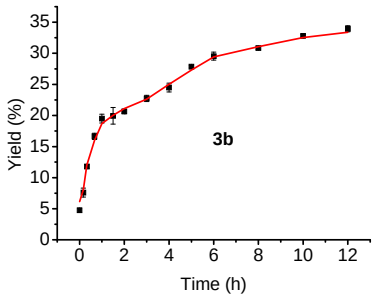

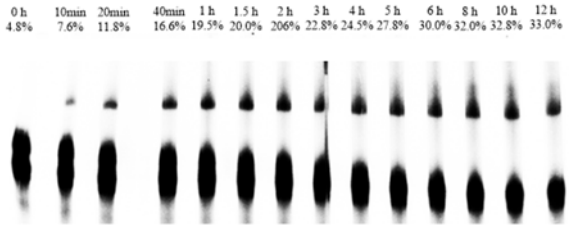

Figure S10. The time dependence of DNA ICL formation of duplex **13** for **3b** (500 μM) upon 350 nm irradiation.

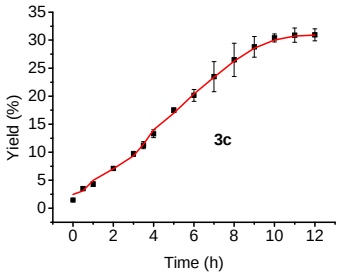

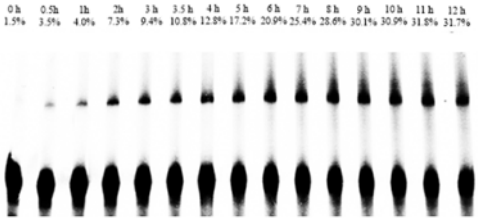

Figure S11. The time dependence of DNA ICL formation of duplex **13** for **3c** (500 μM) upon 350 nm irradiation.

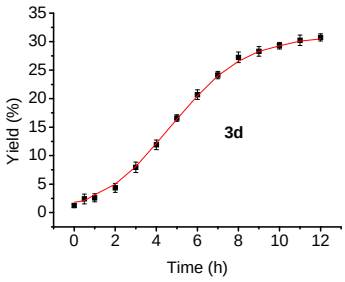

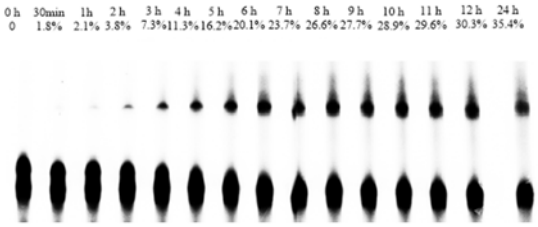

Figure S12. The time dependence of DNA ICL formation of duplex **13** for **3d** (500 μM) upon 350 nm irradiation.

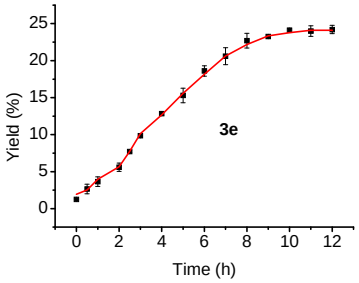

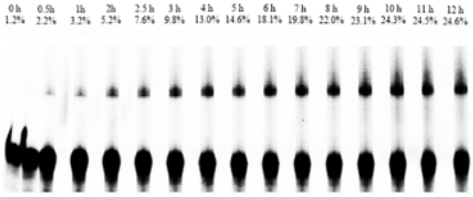

Figure S13. The time dependence of DNA ICL formation of duplex **13** for **3e** (500 μM) upon 350 nm irradiation.

5. Concentration dependent DNA ICL formation.

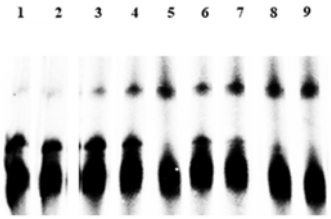

Figure S14. The concentration dependence of DNA ICL formation of duplex **13** for **2a** upon 350 nm irradiation. Lane 1: with DNA only (cross-linking yield 5.6%); lane 2: 10 μM **2a** (6.7%); lane 3: 20 μM **2a** (8.7%); lane 4: 50 μM **2a** (13.2%); lane 5: 100 μM **2a** (19.1%); lane 6: 200 μM **2a** (24.0%); lane 7: 500 μM **2a** (29.2%); lane 8: 1 mM **2a** (30.4%); lane 9: 2 mM **2a** (31.2%). Condition: duplex **13** was irradiated by 350 nm light for 8 h.

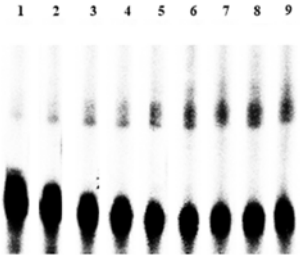

Figure S15. The concentration dependence of DNA ICL formation of duplex **13** for **2b** upon 350 nm irradiation. Lane 1: with DNA only (cross-linking yield 5.4%); lane 2: 10 μM **2b** (11.9%); lane 3: 20 μM **2b** (14.3%); lane 4: 50 μM **2b** (16.8%); lane 5: 100 μM **2b** (21.7%); lane 6: 200 μM **2b** (24.1%); lane 7: 500 μM **2b** (29.8%); lane 8: 1 mM **2b** (29.8%); lane 9: 2 mM **2b** (30.0%). Condition: duplex **13** was irradiated by 350 nm light for 8h.

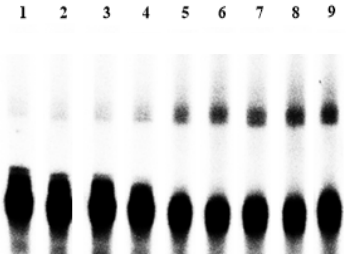

Figure S16. The concentration dependence of DNA ICL formation of duplex **13** for **2c** upon 350 nm irradiation. Lane 1: with DNA only (cross-linking yield 5.7%); lane 2: 10 μM **2c** (6.6%); lane 3: 20 μM **2c** (7.6%); lane 4: 50 μM **3a** (9.8%); lane 5: 100 μM **2c** (12.7%); lane 6: 200 μM **2c** (17.8%); lane 7: 500 μM **3a** (22.9%); lane 8: 1 mM **2c** (22.4%); lane 9: 2 mM **2c** (22.5%). Condition: duplex **13** was irradiated by 350 nm light for 8h.

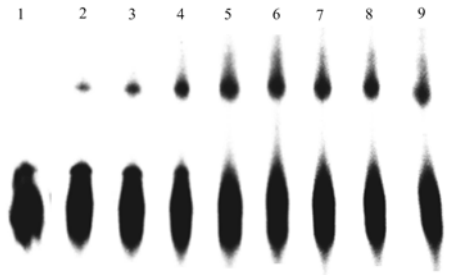

Figure S17. The concentration dependence of DNA ICL formation of duplex **13** for **2d** upon 350 nm irradiation. Lane 1: with DNA only (cross-linking yield 2.6%); lane 2: 10 μM **2d** (7.2%); lane 3: 20 μM **2d** (8.9%); lane 4: 50 μM **2d** (15.8%); lane 5: 100 μM **2d** (23.9%); lane 6: 200 μM **2d** (24.7%); lane 7: 500 μM **2d** (25.6%); lane 8: 1 mM **2d** (25.8%); lane 9: 2 mM **2d** (26.3%). Condition: duplex **13** was irradiated by 350 nm light for 8h.

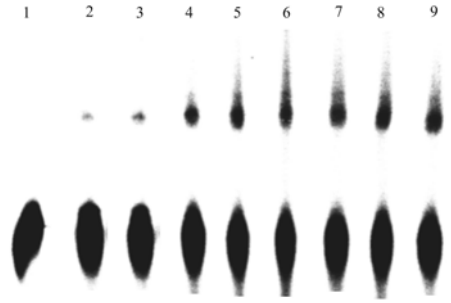

Figure S18. The concentration dependence of DNA ICL formation of duplex **13** for **2e** upon 350 nm irradiation. Lane 1: with DNA only (cross-linking yield 2.6%); lane 2: 10 μM **2e** (4.6%); lane 3: 20 μM **2e** (6.2%); lane 4: 50 μM **2e** (13.8%); lane 5: 100 μM **2e** (21.8%); lane 6: 200 μM **2e** (26.8%); lane 7: 500 μM **2e** (28.0%); lane 8: 1 mM **2e** (27.5%); lane 9: 2 mM **2e** (27.5%). Condition: duplex **13** was irradiated by 350 nm light for 8h.

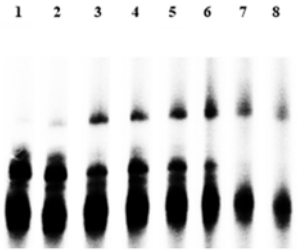

Figure S19. The concentration dependence of DNA ICL formation of duplex **13** for **3a** upon 350 nm irradiation. Lane 1: with DNA only (cross-linking yield 2.3%); lane 2: 10 μM **3a** (3.8%); lane 3: 20 μM **3a** (6.5%); lane 4: 50 μM **3a** (12.0%); lane 5: 100 μM **3a** (17.5%); lane 6: 200 μM **3a** (24.6%); lane 7: 500 μM **3a** (33.2%); lane 8: 1 mM **3a** (37.0%). Condition: duplex **13** was irradiated by 350 nm light for 8h.

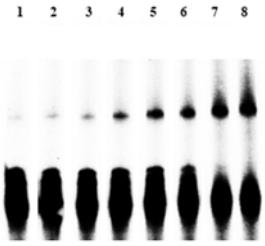

Figure S20. The concentration dependence of DNA ICL formation of duplex **13** for **3b** upon 350 nm irradiation. Lane 1: with DNA only (cross-linking yield 0.1%); lane 2: 10 μM **3b** (4.4%); lane 3: 20 μM **3b** (8.8%); lane 4: 50 μM **3b** (12.8%); lane 5: 100 μM **3b** (20.0%); lane 6: 200 μM **3b** (30.2%); lane 7: 500 μM **3b** (35.2%); lane 8: 1 mM **3b** (38.3%). Condition: duplex **13** was irradiated by 350 nm light for 8h.

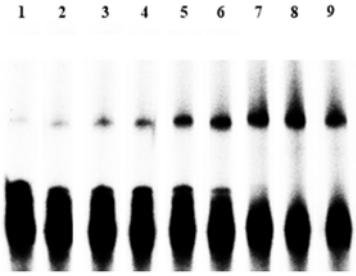

Figure S21. The concentration dependence of DNA ICL formation of duplex **13** for **3c** upon 350 nm irradiation. Lane 1: with DNA only (cross-linking yield 1.9%); lane 2: 10 μM **3c** (2.8%); lane 3: 20 μM **3c** (3.8%); lane 4: 50 μM **3c** (5.6%); lane 5: 100 μM **3c** (8.4%); lane 6: 200 μM **3c** (10.6%); lane 7: 500 μM **3c** (18.6%); lane 8: 1 mM **3c** (23.9%); lane 9: 2 mM **3c** (21.4%). Condition: duplex **13** was irradiated by 350 nm light for 8h.

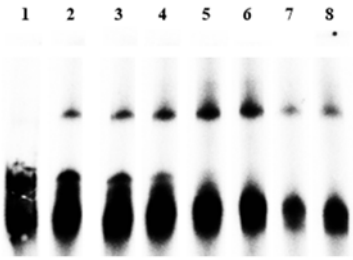

Figure S22. The concentration dependence of DNA ICL formation of duplex **13** for **3d** upon 350 nm irradiation. Lane 1: with DNA only (cross-linking yield 2.4%); lane 2: 10 μM **3d** (6.2%); lane 3: 20 μM **3d** (7.6%); lane 4: 50 μM **3d** (12.0%); lane 5: 100 μM **3d** (20.4%); lane 6: 200 μM **3d** (23.8%); lane 7: 500 μM **3d** (25.2%); lane 8: 1 mM **3d** (27.4%). Condition: duplex **13** was irradiated by 350 nm light for 8h.

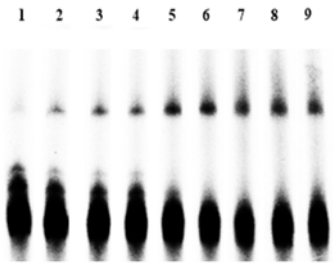

Figure S23. The concentration dependence of DNA ICL formation of duplex **13** for **3e** upon 350 nm irradiation. Lane 1: with DNA only (cross-linking yield 5.3%); lane 2: 10 μM **3e** (8.3%); lane 3: 20 μM **3e** (9.7%); lane 4: 50 μM **3e** (12.6%); lane 5: 100 μM **3e** (19.0%); lane 6: 200 μM **3e** (23.9%); lane 7: 500 μM **3e** (26.2%); lane 8: 1 mM **3e** (28.7%); lane 9: 2 mM **3e** (28.0%). Condition: duplex **13** was irradiated by 350 nm light for 8h.

6. $MeONH_2$ and TEMPO trapping assay

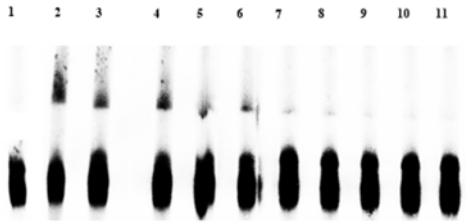

Figure S24. Representative gel of the effect of TEMPO on DNA cross-link formation induced by **2a** upon UV irradiation. Lane 1: with DNA only; lane 2: 0.5 mM **2a** (cross-linking yield 22.4%); lane 3: 0.5 mM **2a** and 0.25 mM TEMPO (15.0%); lane 4: 0.5 mM **2a** and 0.5 mM TEMPO (13.0%); lane 5: 0.5 mM **2a** and 1 mM TEMPO (11.2%); lane 6: 0.5 mM **2a** and 2 mM TEMPO (8.4%); lane 7: 0.5 mM **2a** and 5 mM TEMPO (3.6%); lane 8: 0.5 mM **2a** and 10 mM TEMPO (3.2%); lane 9: 0.5 mM **2a** and 20 mM TEMPO (2.2%); lane 10: 0.5 mM **2a** and 50 mM TEMPO (1.2%); lane 11: 0.5 mM **2a** and 100 mM TEMPO (0.6%). Condition: duplex **13** was irradiated by 350 nm light for 8 h.

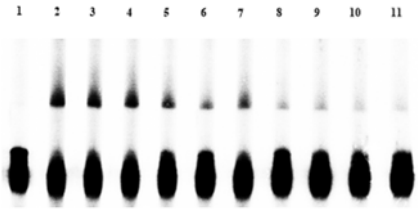

Figure S25. Representative gel of the effect of methoxyamine on DNA cross-link formation induced by **2a** upon UV irradiation. Lane 1: with DNA only; lane 2: 0.5 mM **2a** (cross-linking yield 16.8%); lane 3: 0.5 mM **2a** and 0.25 mM methoxyamine (15.8%); lane 4: 0.5 mM **2a** and 0.5 mM methoxyamine (14.6%); lane 5: 0.5 mM **2a** and 1 mM methoxyamine (14.0%); lane 6: 0.5 mM **2a** and 2 mM methoxyamine (8.9%); lane 7: 0.5 mM **2a** and 5 mM methoxyamine (6.0%); lane 8: 0.5 mM **2a** and 10 mM methoxyamine (4.8%); lane 9: 0.5 mM **2a** and 20 mM methoxyamine (5.0%); lane 10: 0.5 mM **2a** and 50 mM methoxyamine (4.0%); lane 11: 0.5 mM **2a** and 100 mM methoxyamine (2.7%). Condition: duplex **13** was irradiated by 350 nm light for 8 h.

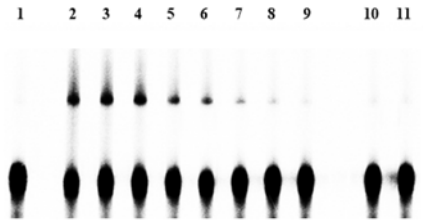

Figure S26. Representative gel of the effect of TEMPO on DNA cross-link formation induced by **2b** upon UV irradiation. Lane 1: with DNA only; lane 2: 0.5 mM **2b** (cross-linking yield 28.7%); lane 3: 0.5 mM **2b** and 0.25 mM TEMPO (21.3%); lane 4: 0.5 mM **2b** and 0.5 mM TEMPO (17.7%); lane 5: 0.5 mM **2b** and 1 mM TEMPO (15.4%); lane 6: 0.5 mM **2b** and 2 mM TEMPO (9.8%); lane 7: 0.5 mM **2b** and 5 mM TEMPO (5.2%); lane 8: 0.5 mM **2b** and 10 mM TEMPO (4.2%); lane 9: 0.5 mM **2b** and 20 mM TEMPO (3.6%); lane 10: 0.5 mM **2b** and 50 mM TEMPO (3.2%); lane 11: 0.5 mM **2b** and 100 mM TEMPO (3.2%). Condition: duplex **13** was irradiated by 350 nm light for 8 h.

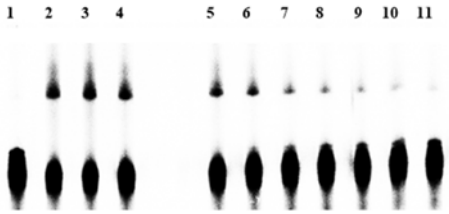

Figure S27. Representative gel of the effect of methoxyamine on DNA cross-link formation induced by **2b** upon UV irradiation. Lane 1: with DNA only; lane 2: 0.5 mM **2b** (cross-linking yield 24.9%); lane 3: 0.5 mM **2b** and 0.25 mM methoxyamine (21.5%); lane 4: 0.5 mM **2b** and 0.5 mM methoxyamine (19.2%); lane 5: 0.5 mM **2b** and 1 mM methoxyamine (17.4%); lane 6: 0.5 mM **2b** and 2 mM methoxyamine (12.1%); lane 7: 0.5 mM **2b** and 5 mM methoxyamine (6.8%); lane 8: 0.5 mM **2b** and 10 mM methoxyamine (5.6%); lane 9: 0.5 mM **2b** and 20 mM methoxyamine (5.2%); lane 10: 0.5 mM **2b** and 50 mM methoxyamine (4.9%); lane 11: 0.5 mM **2b** and 100 mM methoxyamine (3.9%). Condition: duplex **13** was irradiated by 350 nm light for 8 h.

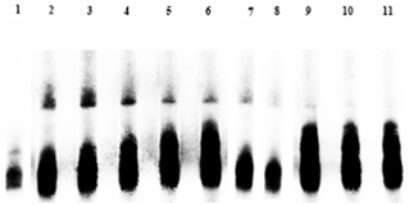

Figure S28. Representative gel of the effect of TEMPO on DNA cross-link formation induced by **2c** upon UV irradiation. Lane 1: with DNA only; lane 2: 0.5 mM **2c** (cross-linking yield 18.9%); lane 3: 0.5 mM **2c** and 0.25 mM TEMPO (14.2%); lane 4: 0.5 mM **2c** and 0.5 mM TEMPO (14.0%); lane 5: 0.5 mM **2c** and 1 mM TEMPO (13.8%); lane 6: 0.5 mM **2c** and 2 mM TEMPO (13.0%); lane 7: 0.5 mM **2c** and 5 mM TEMPO (6.7%); lane 8: 0.5 mM **2c** and 10 mM TEMPO (4.6%); lane 9: 0.5 mM **2c** and 20 mM TEMPO (3.8%); lane 10: 0.5 mM **2c** and 50 mM TEMPO (3.7%); lane 11: 0.5 mM **2c** and 100 mM TEMPO (3.0%). Condition: duplex **13** was irradiated by 350 nm light for 8 h.

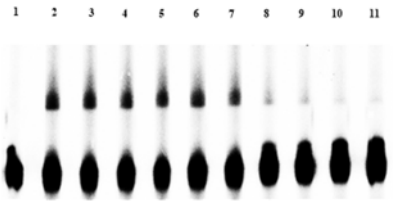

Figure S29. Representative gel of the effect of methoxyamine on DNA cross-link formation induced by **2c** upon UV irradiation. Lane 1: with DNA only; lane 2: 0.5 mM **2c** (cross-linking yield 22.6%); lane 3: 0.5 mM **2c** and 0.25 mM methoxyamine (20.6%); lane 4: 0.5 mM **2c** and 0.5 mM methoxyamine (18.8%); lane 5: 0.5 mM **2c** and 1 mM methoxyamine (16.2%); lane 6: 0.5 mM **2c** and 2 mM methoxyamine (15.0%); lane 7: 0.5 mM **2c** and 5 mM methoxyamine (13.0%); lane 8: 0.5 mM **2c** and 10 mM methoxyamine (3.4%); lane 9: 0.5 mM **2c** and 20 mM methoxyamine (1.2%); lane 10: 0.5 mM **2c** and 50 mM methoxyamine (0.5%); lane 11: 0.5 mM **2c** and 100 mM methoxyamine (0.4%). Condition: duplex **13** was irradiated by 350 nm light for 8 h.

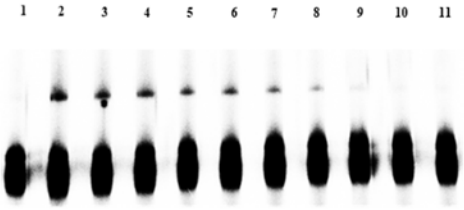

Figure S30. Representative gel of the effect of TEMPO on DNA cross-link formation induced by **2d** upon UV irradiation. Lane 1: with DNA only; lane 2: 0.5 mM **2d** (cross-linking yield 13.3%); lane 3: 0.5 mM **2d** and 0.25 mM TEMPO (8.3%); lane 4: 0.5 mM **2d** and 0.5 mM TEMPO (7.6%); lane 5: 0.5 mM **2d** and 1 mM TEMPO (5.1%); lane 6: 0.5 mM **2d** and 2 mM TEMPO (4.3%); lane 7: 0.5 mM **2d** and 5 mM TEMPO (3.6%); lane 8: 0.5 mM **2d** and 10 mM TEMPO (2.9%); lane 9: 0.5 mM **2d** and 20 mM TEMPO (3.0%); lane 10: 0.5 mM **2d** and 50 mM TEMPO (1.2%); lane 11: 0.5 mM **2d** and 100 mM TEMPO (0.65%). Condition: duplex **13** was irradiated by 350 nm light for 8 h.

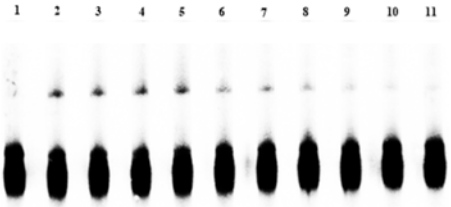

Figure S31. Representative gel of the effect of methoxyamine on DNA cross-link formation induced by **2d** upon UV irradiation. Lane 1: with DNA only; lane 2: 0.5 mM **2d** (cross-linking yield 12.2%); lane 3: 0.5 mM **2d** and 0.25 mM methoxyamine (7.5%); lane 4: 0.5 mM **2d** and 0.5 mM methoxyamine (6.0%); lane 5: 0.5 mM **2d** and 1 mM methoxyamine (5.2%); lane 6: 0.5 mM **2d** and 2 mM methoxyamine (5.2%); lane 7: 0.5 mM **2d** and 5 mM methoxyamine (4.2%); lane 8: 0.5 mM **2d** and 10 mM methoxyamine (3.4%); lane 9: 0.5 mM **2d** and 20 mM methoxyamine (3.0%); lane 10: 0.5 mM **2d** and 50 mM methoxyamine (2.1%); lane 11: 0.5 mM **2d** and 100 mM methoxyamine (2%). Condition: duplex **13** was irradiated by 350 nm light for 8 h.

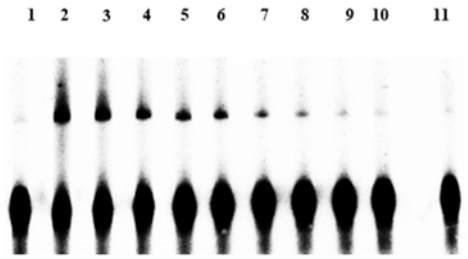

Figure S32. Representative gel of the effect of TEMPO on DNA cross-link formation induced by **2e** upon UV irradiation. Lane 1: with DNA only; lane 2: 0.5 mM **2e** (cross-linking yield 30.4%); lane 3: 0.5 mM **2e** and 0.25 mM TEMPO (18.4%); lane 4: 0.5 mM **2e** and 0.5 mM TEMPO (14.5%); lane 5: 0.5 mM **2e** and 1 mM TEMPO (8.8%); lane 6: 0.5 mM **2e** and 2 mM TEMPO (7.9%); lane 7: 0.5 mM **2e** and 5 mM TEMPO (5.6%); lane 8: 0.5 mM **2e** and 10 mM TEMPO (4.4%); lane 9: 0.5 mM **2e** and 20 mM TEMPO (3.4%); lane 10: 0.5 mM **2e** and 50 mM TEMPO (3.3%); lane 11: 0.5 mM **2e** and 100 mM TEMPO (3.2%). Condition: duplex **13** was irradiated by 350 nm light for 8 h.

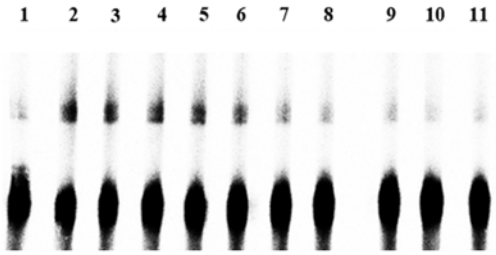

Figure S33. Representative gel of the effect of methoxyamine on DNA cross-link formation induced by **2e** upon UV irradiation. Lane 1: with DNA only; lane 2: 0.5 mM **2e** (cross-linking yield 23.8%); lane 3: 0.5 mM **2e** and 0.25 mM methoxyamine (18.4%); lane 4: 0.5 mM **2e** and 0.5 mM methoxyamine (16.8%); lane 5: 0.5 mM **2e** and 1 mM methoxyamine (16.3%); lane 6: 0.5 mM **2e** and 2 mM methoxyamine (13.0%); lane 7: 0.5 mM **2e** and 5 mM methoxyamine (9.0%); lane 8: 0.5 mM **2e** and 10 mM methoxyamine (7.8%); lane 9: 0.5 mM **2e** and 20 mM methoxyamine (4.2%); lane 10: 0.5 mM **2e** and 50 mM methoxyamine (3.8%); lane 11: 0.5 mM **2e** and 100 mM methoxyamine (3.4%). Condition: duplex **13** was irradiated by 350 nm light for 8 h.

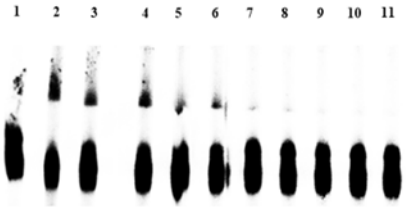

Figure S34. Representative gel of the effect of TEMPO on DNA cross-link formation induced by **3a** upon UV irradiation. Lane 1: with DNA only; lane 2: 0.5 mM **3a** (cross-linking yield 27.2%); lane 3: 0.5 mM **3a** and 0.25 mM TEMPO (24.0%); lane 4: 0.5 mM **3a** and 0.5 mM TEMPO (18.2%); lane 5: 0.5 mM **3a** and 1 mM TEMPO (10.2%); lane 6: 0.5 mM **3a** and 2 mM TEMPO (8.1%); lane 7: 0.5 mM **3a** and 5 mM TEMPO (3.6%); lane 8: 0.5 mM **3a** and 10 mM TEMPO (2.4%); lane 9: 0.5 mM **3a** and 20 mM TEMPO (1.9%); lane 10: 0.5 mM **3a** and 50 mM TEMPO (1.5%); lane 11: 0.5 mM **3a** and 100 mM TEMPO (1.4%). Condition: duplex **13** was irradiated by 350 nm light for 8 h.

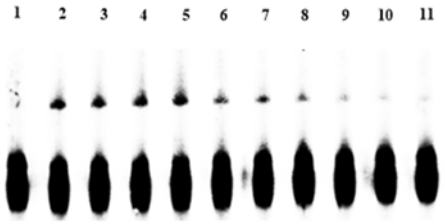

Figure S35. Representative gel of the effect of methoxyamine on DNA cross-link formation induced by **3a** upon UV irradiation. Lane 1: with DNA only; lane 2: 0.5 mM **3a** (cross-linking yield 26.0%); lane 3: 0.5 mM **3a** and 0.25 mM methoxyamine (20.8%); lane 4: 0.5 mM **3a** and 0.5 mM methoxyamine (19.2%); lane 5: 0.5 mM **3a** and 1 mM methoxyamine (17.2%); lane 6: 0.5 mM **3a** and 2 mM methoxyamine (11.2%); lane 7: 0.5 mM **3a** and 5 mM methoxyamine (6.9%); lane 8: 0.5 mM **3a** and 10 mM methoxyamine (3.6%); lane 9: 0.5 mM **3a** and 20 mM methoxyamine (1.7%); lane 10: 0.5 mM **3a** and 50 mM methoxyamine (0.7%); lane 11: 0.5 mM **3a** and 100 mM methoxyamine (0.4%). Condition: duplex **13** was irradiated by 350 nm light for 8 h.

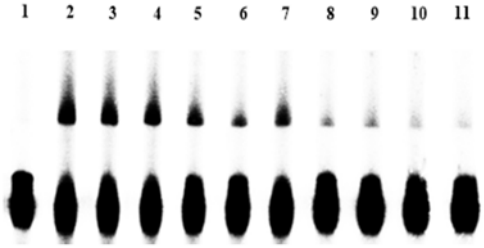

Figure S36. Representative gel of the effect of TEMPO on DNA cross-link formation induced by **3b** upon UV irradiation. Lane 1: with DNA only; lane 2: 0.5 mM **3b** (cross-linking yield 32.8%); lane 3: 0.5 mM **3b** and 0.25 mM TEMPO (29.6%); lane 4: 0.5 mM **3b** and 0.5 mM TEMPO (25.8%); lane 5: 0.5 mM **3b** and 1 mM TEMPO (19.0%); lane 6: 0.5 mM **3b** and 2 mM TEMPO (13.6%); lane 7: 0.5 mM **3b** and 5 mM TEMPO (9.0%); lane 8: 0.5 mM **3b** and 10 mM TEMPO (5.2%); lane 9: 0.5 mM **3b** and 20 mM TEMPO (4.2%); lane 10: 0.5 mM **3b** and 50 mM TEMPO (2.9%); lane 11: 0.5 mM **3b** and 100 mM TEMPO (2.4%). Condition: duplex **13** was irradiated by 350 nm light for 8 h.

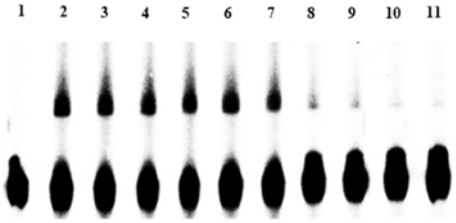

Figure S37. Representative gel of the effect of methoxyamine on DNA cross-link formation induced by **3b** upon UV irradiation. Lane 1: with DNA only; lane 2: 0.5 mM **3b** (cross-linking yield 31.4%); lane 3: 0.5 mM **3b** and 0.25 mM methoxyamine (27.6%); lane 4: 0.5 mM **3b** and 0.5 mM methoxyamine (26.5%); lane 5: 0.5 mM **3b** and 1 mM methoxyamine (23.8%); lane 6: 0.5 mM **3b** and 2 mM methoxyamine (21.6%); lane 7: 0.5 mM **3b** and 5 mM methoxyamine (16.6%); lane 8: 0.5 mM **3b** and 10 mM methoxyamine (7.6%); lane 9: 0.5 mM **3b** and 20 mM methoxyamine (4.0%); lane 10: 0.5 mM **3b** and 50 mM methoxyamine (2.2%); lane 11: 0.5 mM **3b** and 100 mM methoxyamine (1.8%). Condition: duplex **13** was irradiated by 350 nm light for 8 h.

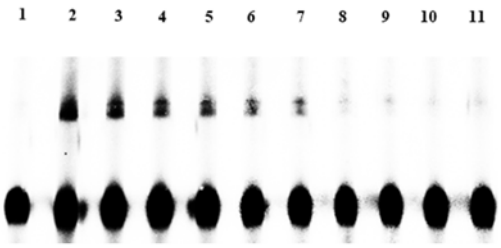

Figure S38. Representative gel of the effect of TEMPO on DNA cross-link formation induced by **3c** upon UV irradiation. Lane 1: with DNA only; lane 2: 0.5 mM **3c** (cross-linking yield 15.2%); lane 3: 0.5 mM **3c** and 0.25 mM TEMPO (9.2%); lane 4: 0.5 mM **3c** and 0.5 mM TEMPO (8.4%); lane 5: 0.5 mM **3c** and 1 mM TEMPO (7.6%); lane 6: 0.5 mM **3c** and 2 mM TEMPO (7.4%); lane 7: 0.5 mM **3c** and 5 mM TEMPO (7.1%); lane 8: 0.5 mM **3c** and 10 mM TEMPO (5.8%); lane 9: 0.5 mM **3c** and 20 mM TEMPO (2.4%); lane 10: 0.5 mM **3c** and 50 mM TEMPO (2.4%); lane 11: 0.5 mM **3c** and 100 mM TEMPO (2.5%). Condition: duplex **13** was irradiated by 350 nm light for 8 h.

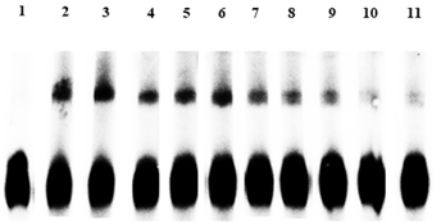

Figure S39. Representative gel of the effect of methoxyamine on DNA cross-link formation induced by **3c** upon UV irradiation. Lane 1: with DNA only; lane 2: 0.5 mM **3c** (cross-linking yield 17.6%); lane 3: 0.5 mM **3c** and 0.25 mM methoxyamine (15.1%); lane 4: 0.5 mM **3c** and 0.5 mM methoxyamine (14.9%); lane 5: 0.5 mM **3c** and 1 mM methoxyamine (12.3%); lane 6: 0.5 mM **3c** and 2 mM methoxyamine (12.0%); lane 7: 0.5 mM **3c** and 5 mM methoxyamine (9.0%); lane 8: 0.5 mM **3c** and 10 mM methoxyamine (7.1%); lane 9: 0.5 mM **3c** and 20 mM methoxyamine (6.3%); lane 10: 0.5 mM **3c** and 50 mM methoxyamine (5.3%); lane 11: 0.5 mM **3c** and 100 mM methoxyamine (2%). Condition: duplex **13** was irradiated by 350 nm light for 8 h.

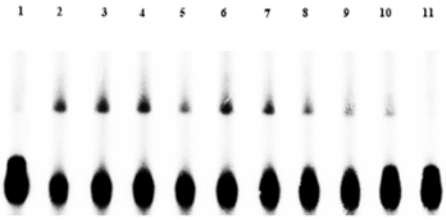

Figure S40. Representative gel of the effect of TEMPO on DNA cross-link formation induced by **3d** upon UV irradiation. Lane 1: with DNA only; lane 2: 0.5 mM **3d** (cross-linking yield 24.6%); lane 3: 0.5 mM **3d** and 0.25 mM TEMPO (15.6%); lane 4: 0.5 mM **3d** and 0.5 mM TEMPO (13.9%); lane 5: 0.5 mM **3d** and 1 mM TEMPO (11.7%); lane 6: 0.5 mM **3d** and 2 mM TEMPO (10.6%); lane 7: 0.5 mM **3d** and 5 mM TEMPO (8.0%); lane 8: 0.5 mM **3d** and 10 mM TEMPO (7.6%); lane 9: 0.5 mM **3d** and 20 mM TEMPO (6.6%); lane 10: 0.5 mM **3d** and 50 mM TEMPO (2.6%); lane 11: 0.5 mM **3d** and 100 mM TEMPO (0.2%). Condition: duplex **13** was irradiated by 350 nm light for 8 h.

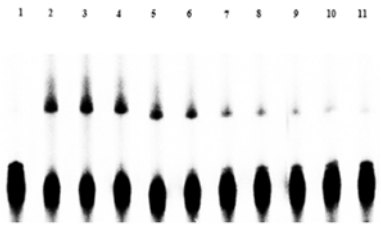

Figure S41. Representative gel of the effect of methoxyamine on DNA cross-link formation induced by **3d** upon UV irradiation. Lane 1: with DNA only; lane 2: 0.5 mM **3d** (cross-linking yield 24.9%); lane 3: 0.5 mM **3d** and 0.25 mM methoxyamine (16.6%); lane 4: 0.5 mM **3d** and 0.5 mM methoxyamine (14.3%); lane 5: 0.5 mM **3d** and 1 mM methoxyamine (12.0%); lane 6: 0.5 mM **3d** and 2 mM methoxyamine (11.4%); lane 7: 0.5 mM **3d** and 5 mM methoxyamine (8.2%); lane 8: 0.5 mM **3d** and 10 mM methoxyamine (8.2%); lane 9: 0.5 mM **3d** and 20 mM methoxyamine (6.4%); lane 10: 0.5 mM **3d** and 50 mM methoxyamine (1.7%); lane 11: 0.5 mM **3d** and 100 mM methoxyamine (1.0%). Condition: duplex **13** was irradiated by 350 nm light for 8 h.

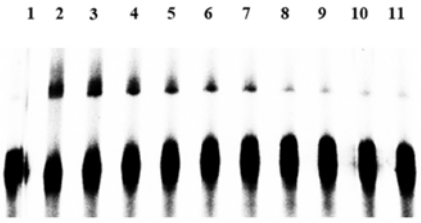

Figure S42. Representative gel of the effect of TEMPO on DNA cross-link formation induced by **3e** upon UV irradiation. Lane 1: with DNA only; lane 2: 0.5 mM **3e** (cross-linking yield 30.8%); lane 3: 0.5 mM **3e** and 0.25 mM TEMPO (25.0%); lane 4: 0.5 mM **3e** and 0.5 mM TEMPO (24.4%); lane 5: 0.5 mM **3e** and 1 mM TEMPO (21.2%); lane 6: 0.5 mM **3e** and 2 mM TEMPO (19.5%); lane 7: 0.5 mM **3e** and 5 mM TEMPO (15.6%); lane 8: 0.5 mM **3e** and 10 mM TEMPO (15.2%); lane 9: 0.5 mM **3e** and 20 mM TEMPO (12.3%); lane 10: 0.5 mM **3e** and 50 mM TEMPO (8.8%); lane 11: 0.5 mM **3e** and 100 mM TEMPO (7.9%). Condition: duplex **13** was irradiated by 350 nm light for 8 h.

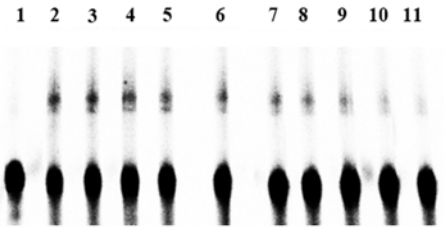

Figure S43. Representative gel of the effect of methoxyamine on DNA cross-link formation induced by **3e** upon UV irradiation. Lane 1: with DNA only; lane 2: 0.5 mM **3e** (cross-linking yield 30.8%); lane 3: 0.5 mM **3e** and 0.25 mM methoxyamine (24.7%); lane 4: 0.5 mM **3e** and 0.5 mM methoxyamine (24.7%); lane 5: 0.5 mM **3e** and 1 mM methoxyamine (21.5%); lane 6: 0.5 mM **3e** and 2 mM methoxyamine (19.4%); lane 7: 0.5 mM **3e** and 5 mM methoxyamine (15.6%); lane 8: 0.5 mM **3e** and 10 mM methoxyamine (15.2%); lane 9: 0.5 mM **3e** and 20 mM methoxyamine (12.5%); lane 10: 0.5 mM **3e** and 50 mM methoxyamine (9.0%); lane 11: 0.5 mM **3e** and 100 mM methoxyamine (7.6%). Condition: duplex **13** was irradiated by 350 nm light for 8 h.

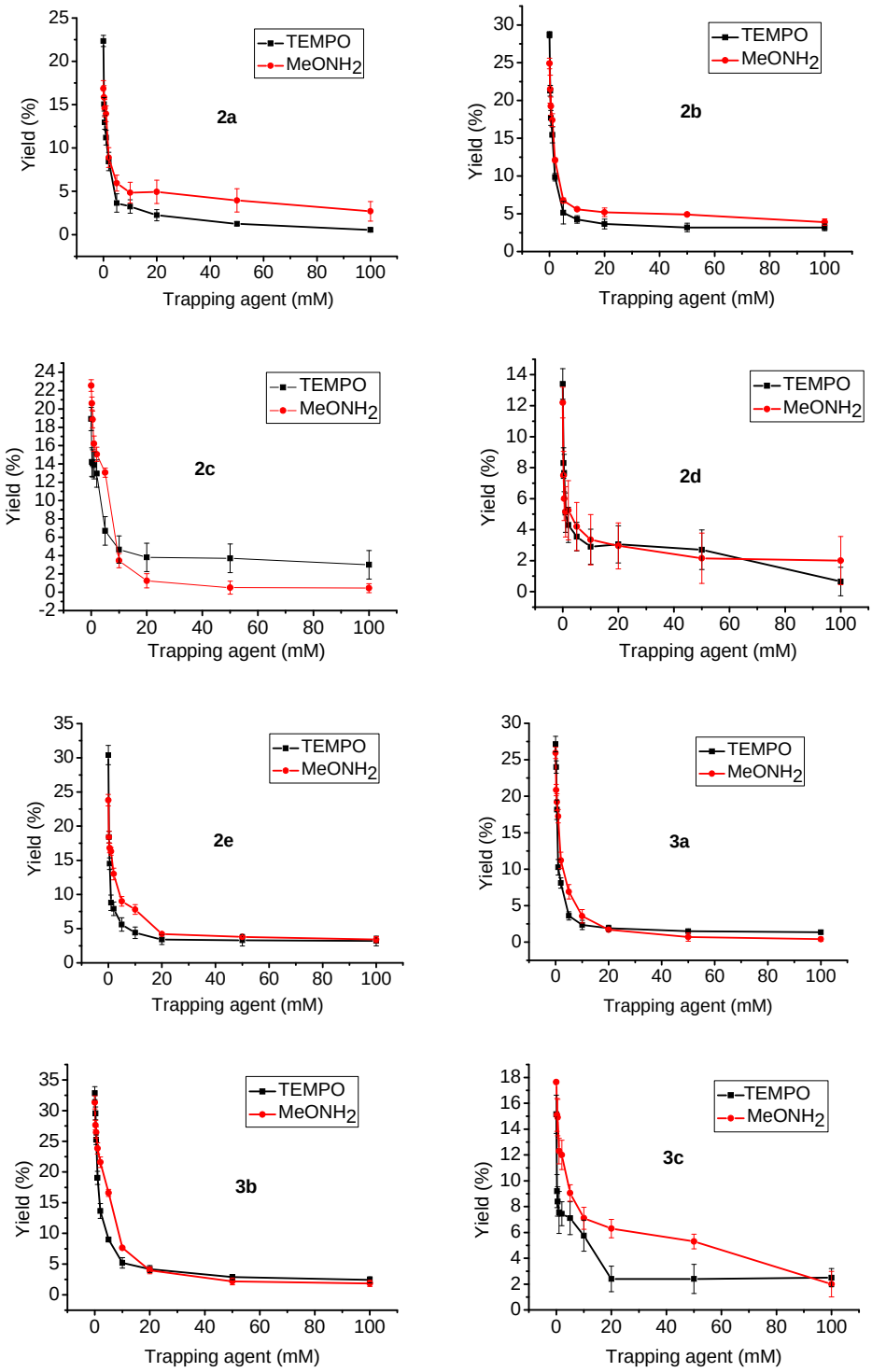
2a
2b
2c
2d
2e
3a
3b
3c
TEMPO
MeONH2
Yield (%)
Trapping agent (mM)

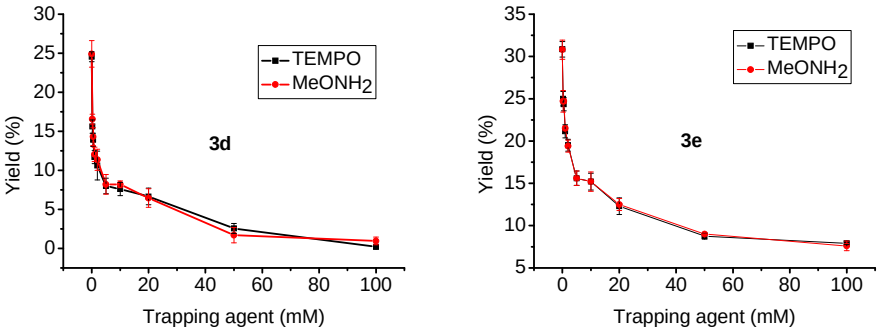

Figure S44. The effect of TEMPO and methoxyamine on DNA ICL formation of duplex **13** for compounds **2a-e** and **3a-e**.

7. Determination of DNA alkylation sites.

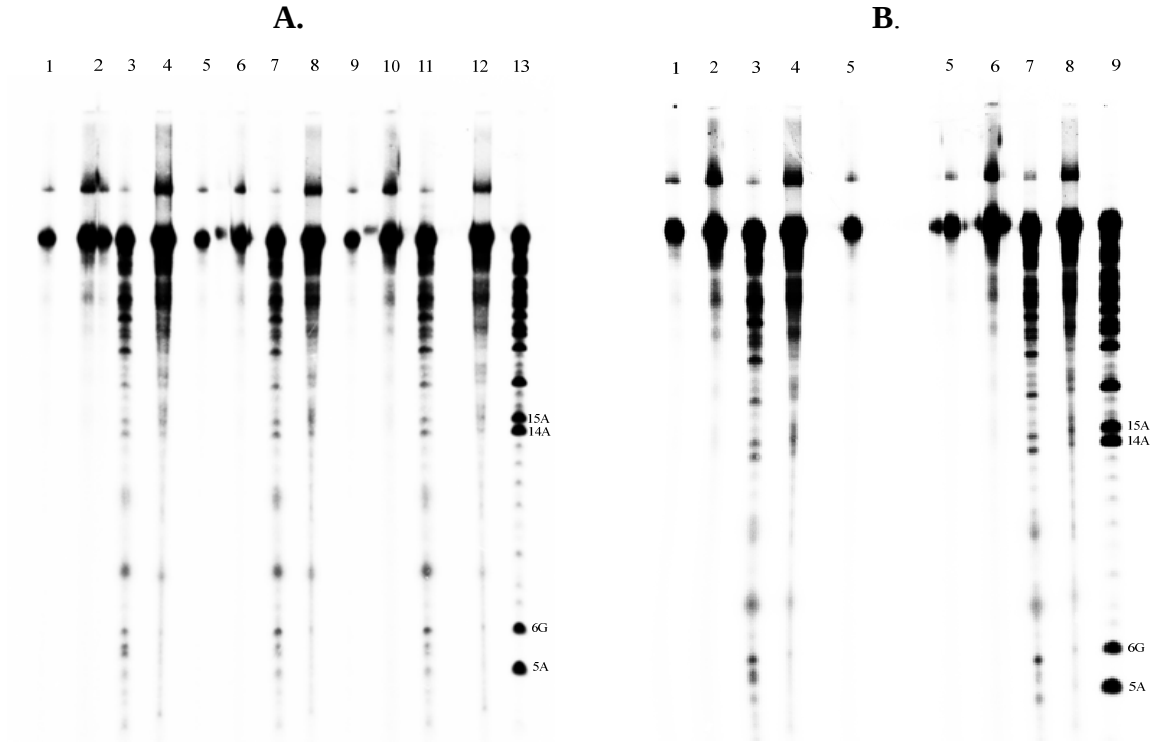

Figure S45. Determination of cross-linking site of **2a-e**. Phosphorimage autoradiogram of 20% denaturing PAGE analysis of the DNA ICL products upon heating in piperidine. (A) compounds **2a-c**: lane 1: **2a**, no precipitation; lane 2: **2a**, control (after precipitation); lane 3: **2a**, heating of ICL in 1.0 M piperidine at 90 °C for 30 min; lane 4: **2a**, heating of ICL in phosphate buffer (pH 7) at 90 °C for 30 min; lane 5: **2b**, no precipitation; lane 6: **2b**, control (after precipitation); lane 7: **2b**, heating of ICL in 1.0 M piperidine at 90 °C for 30 min; lane 8: **2b**, heating of ICL in phosphate buffer (pH 7) at 90 °C for 30 min; lane 9: **2c**, no precipitation; lane 10: **2c**, control (after precipitation); lane 11: **2c**, heating of ICL in 1.0 M piperidine at 90 °C for 30 min; lane 12: **2c**, heating of ICL in phosphate buffer (pH 7) at 90 °C for 30 min; lane 13: G+A sequencing. (B) compounds **2d** and **2e**: lane 1: **2d**, no precipitation; lane 2: **2d**, control (after precipitation); lane 3: **2d**, heating of ICL in 1.0 M piperidine at 90 °C for 30 min; lane 4: **2d**, heating of ICL in phosphate buffer (pH 7) at 90 °C for 30 min; lane 5: **2e**, no precipitation; lane 6: **2e**, control (after precipitation); lane 7: **2e**, heating of ICL in 1.0 M piperidine at 90 °C for 30 min; lane 8: **2e**, heating of ICL in phosphate buffer (pH 7) at 90 °C for 30 min; lane 9: G+A sequencing.

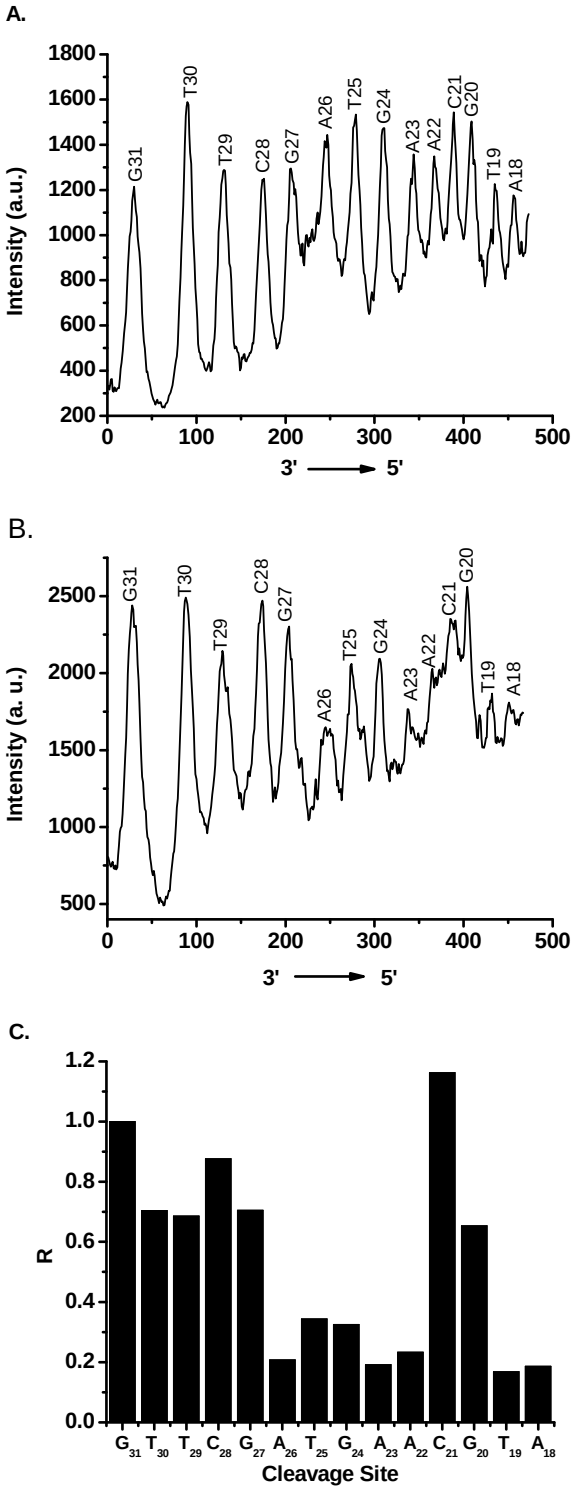

Figure S46. Determination of the interstrand cross-linking position via OH• cleavage of **3b**-cross-linked DNA duplex **27**: (A) partial fragmentation patterns for native duplex **27** using iron(II)/EDTA; (B) partial fragmentation patterns for **3b**-cross-linked **27** using iron(II)/EDTA; (C) ratio of fragment abundance in **3b**-cross-linked and native DNA duplex **27** as a function of the cleavage site. ODN **27a** was ^{32}P-labeled at the 3′-terminus.

8. NMR spectra.

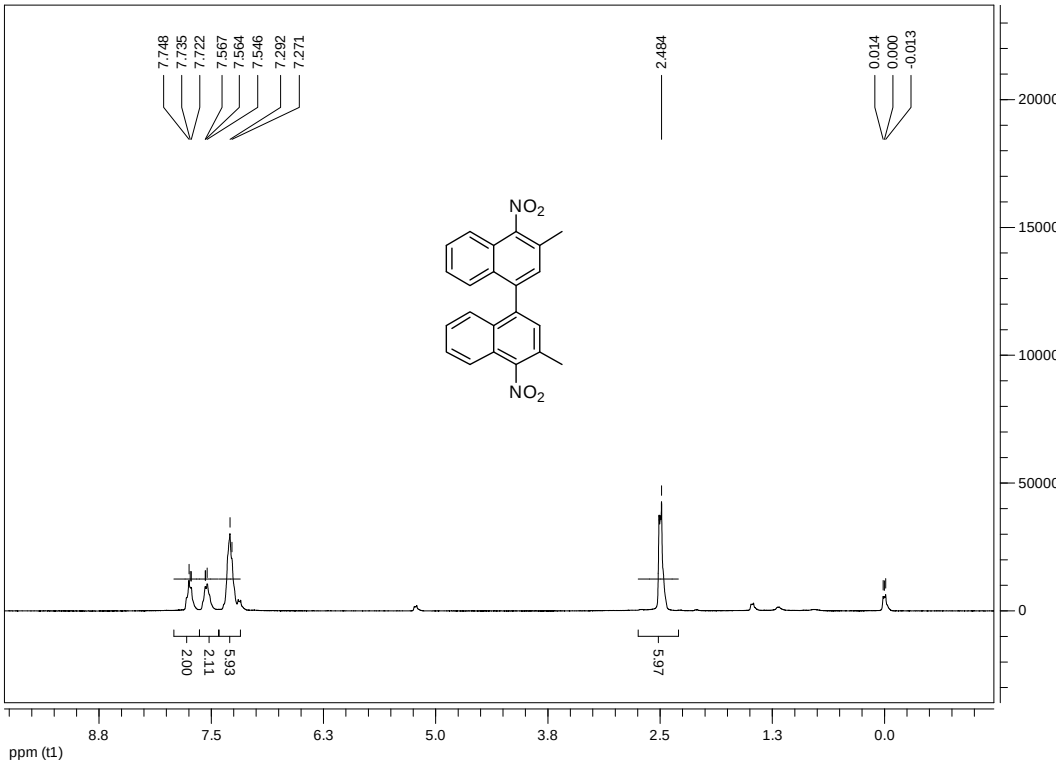

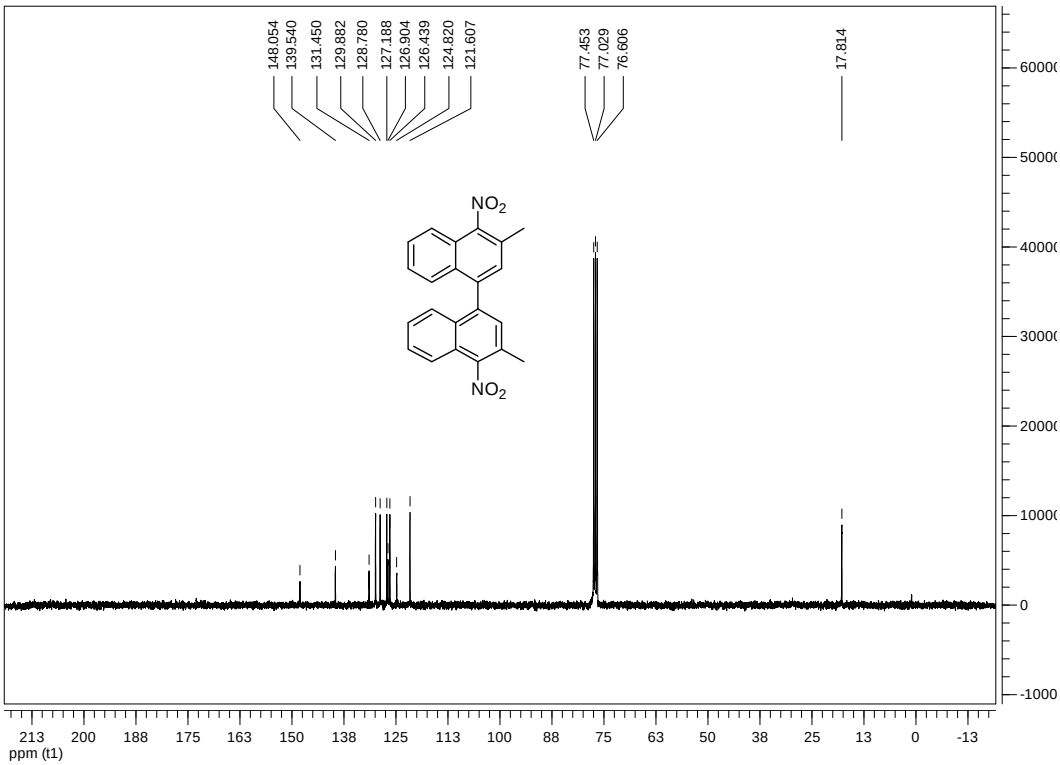

Figure S47. NMR of **11**

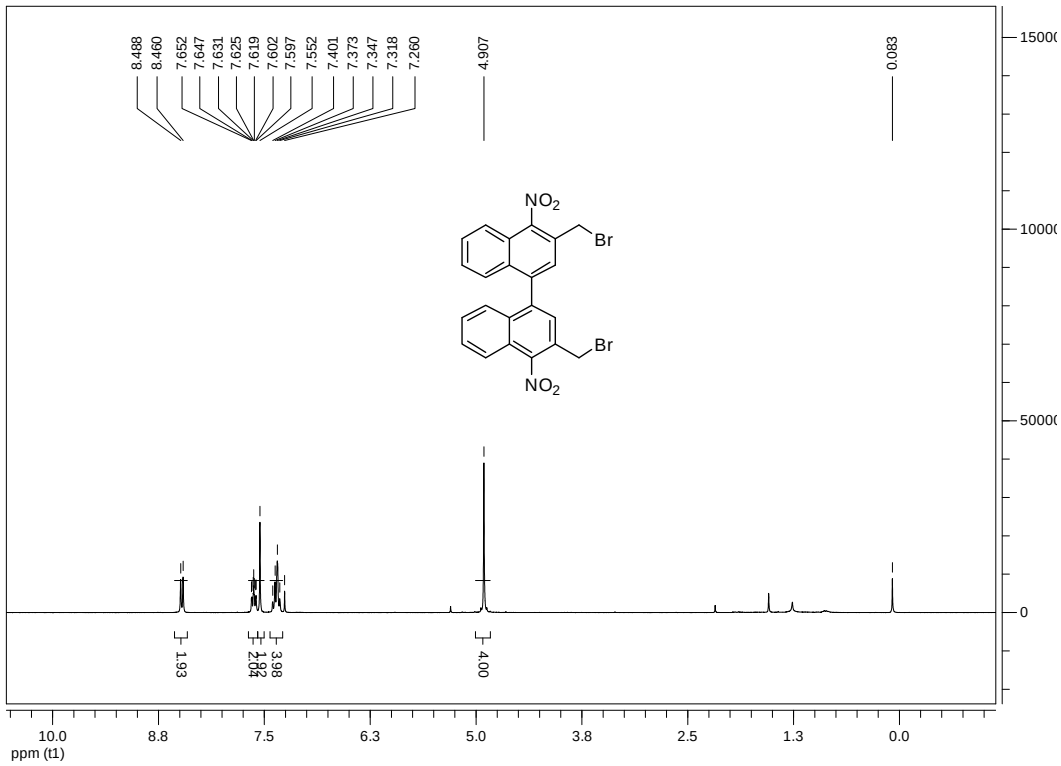

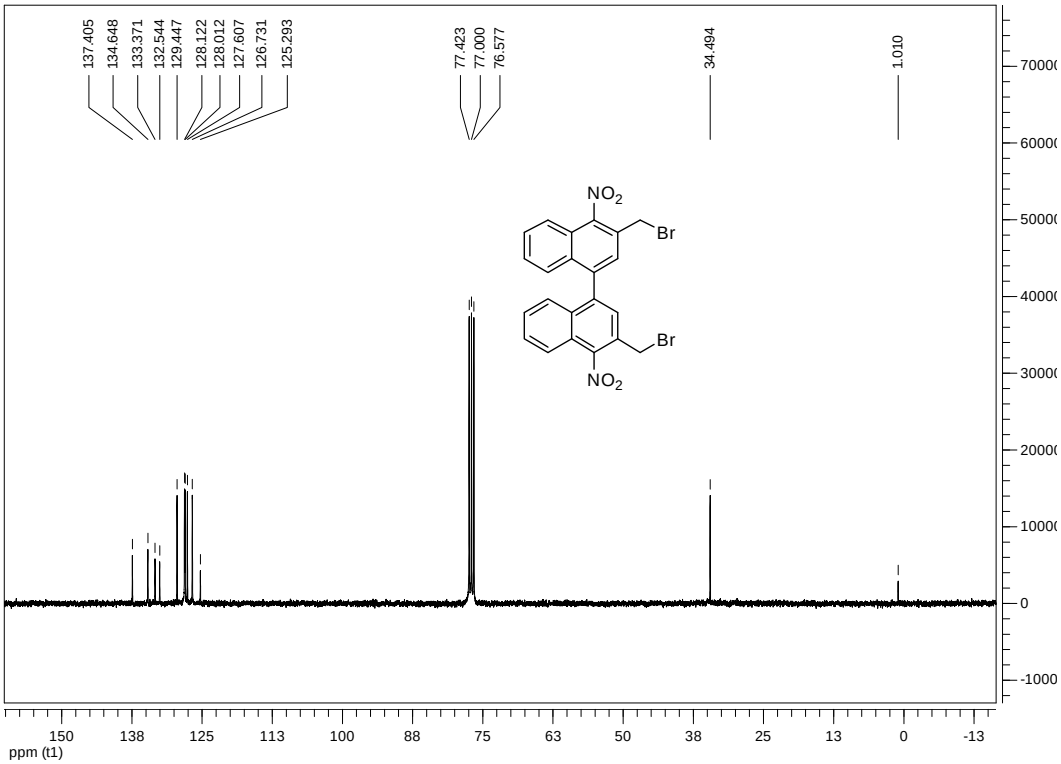

Figure S48. NMR of **2a**

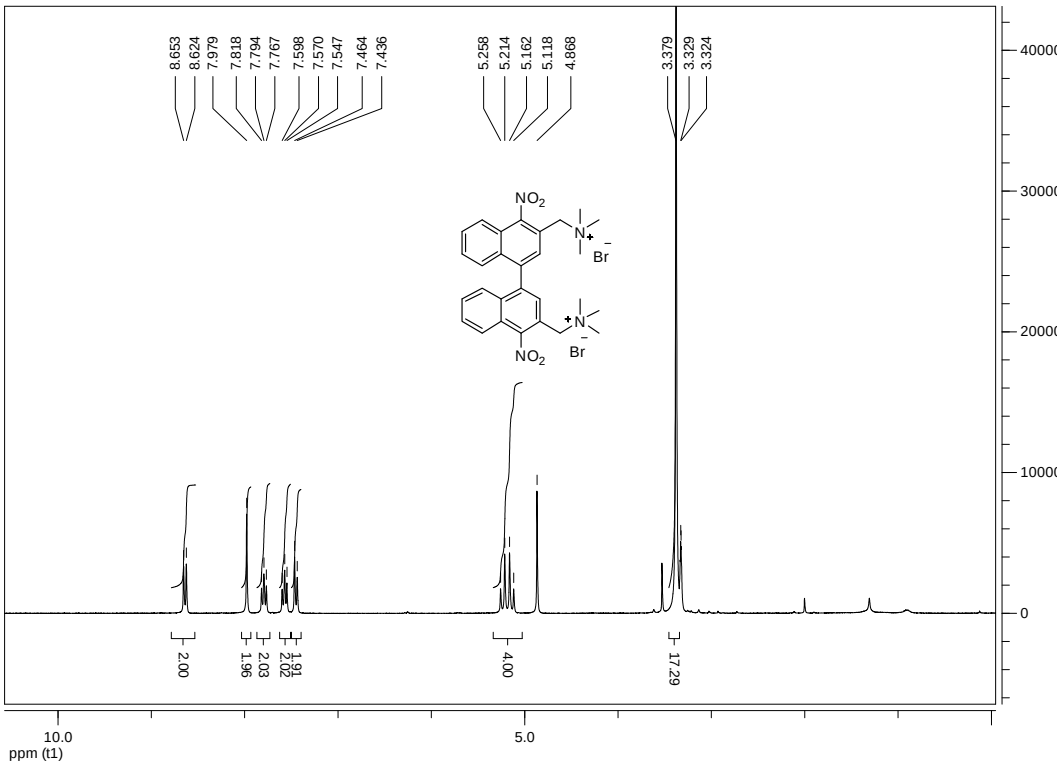

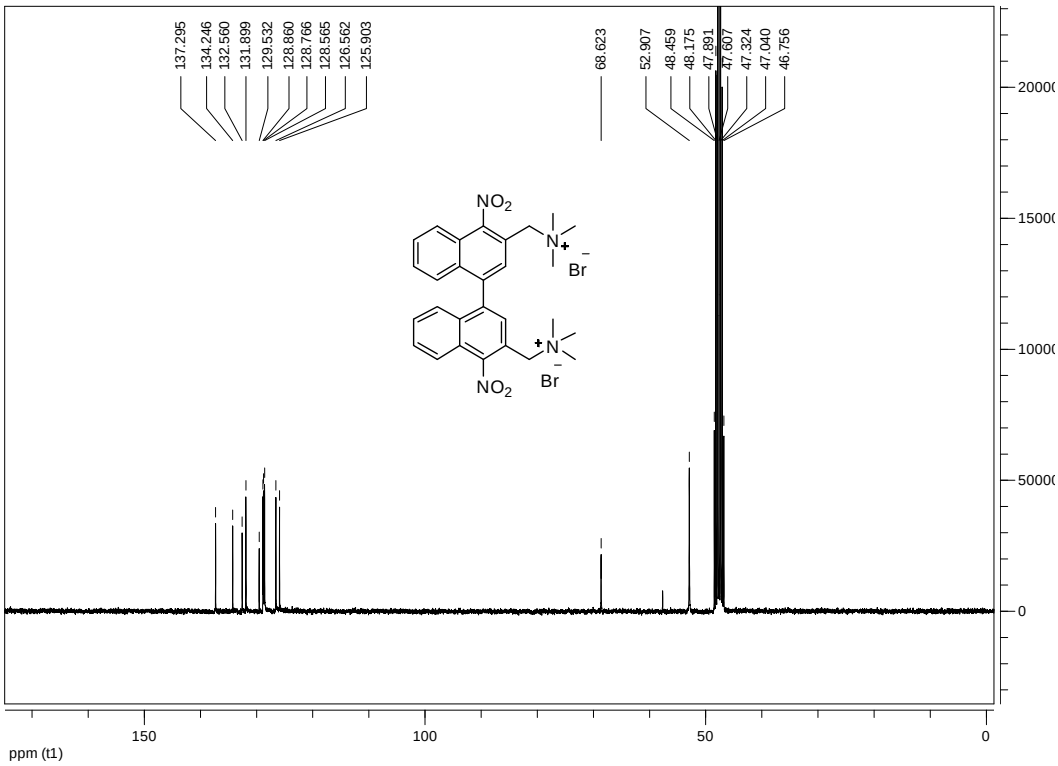

Figure S49. NMR of **3a**

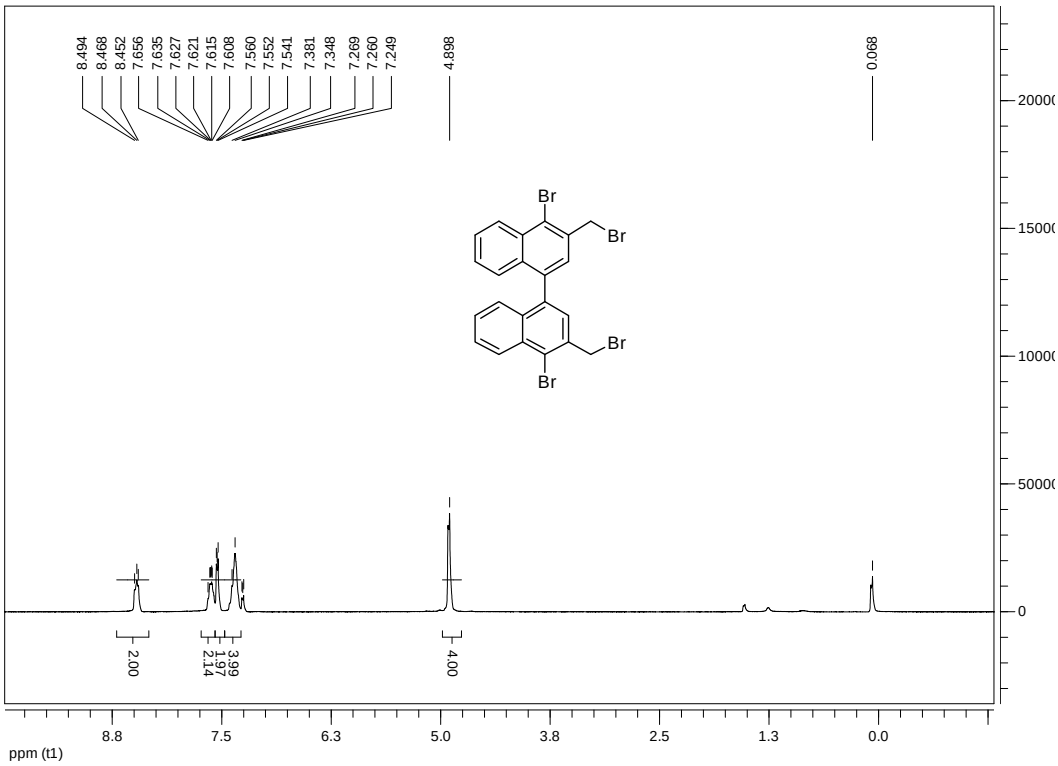

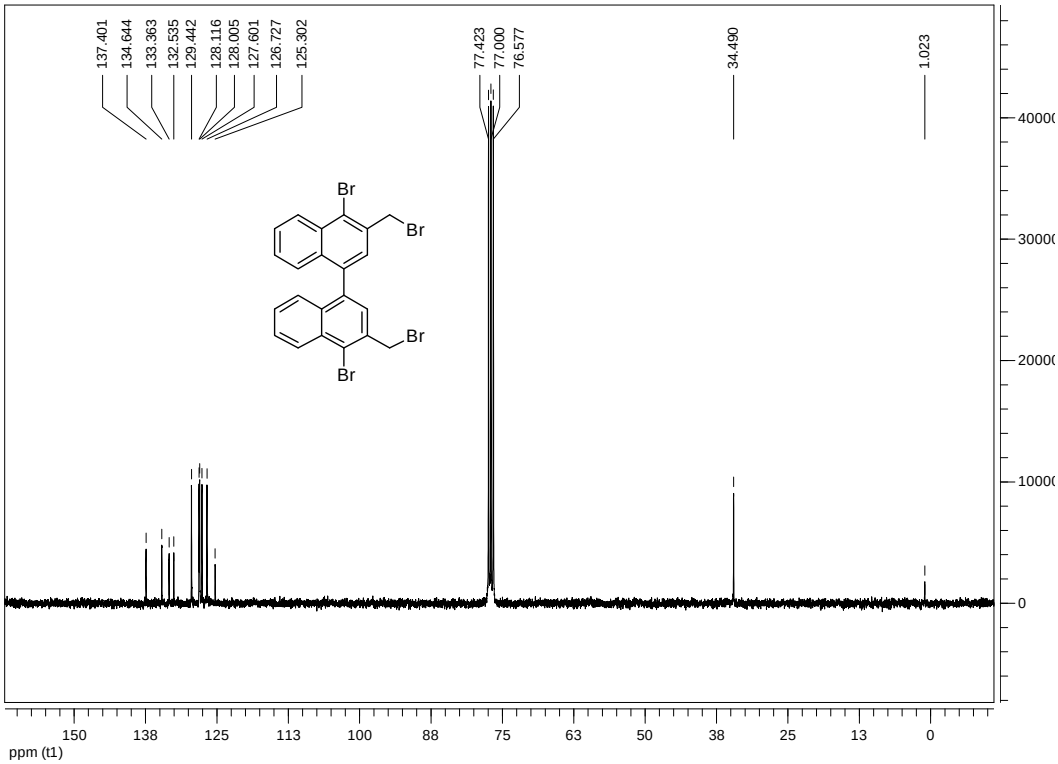

Figure S50. NMR of **2b**

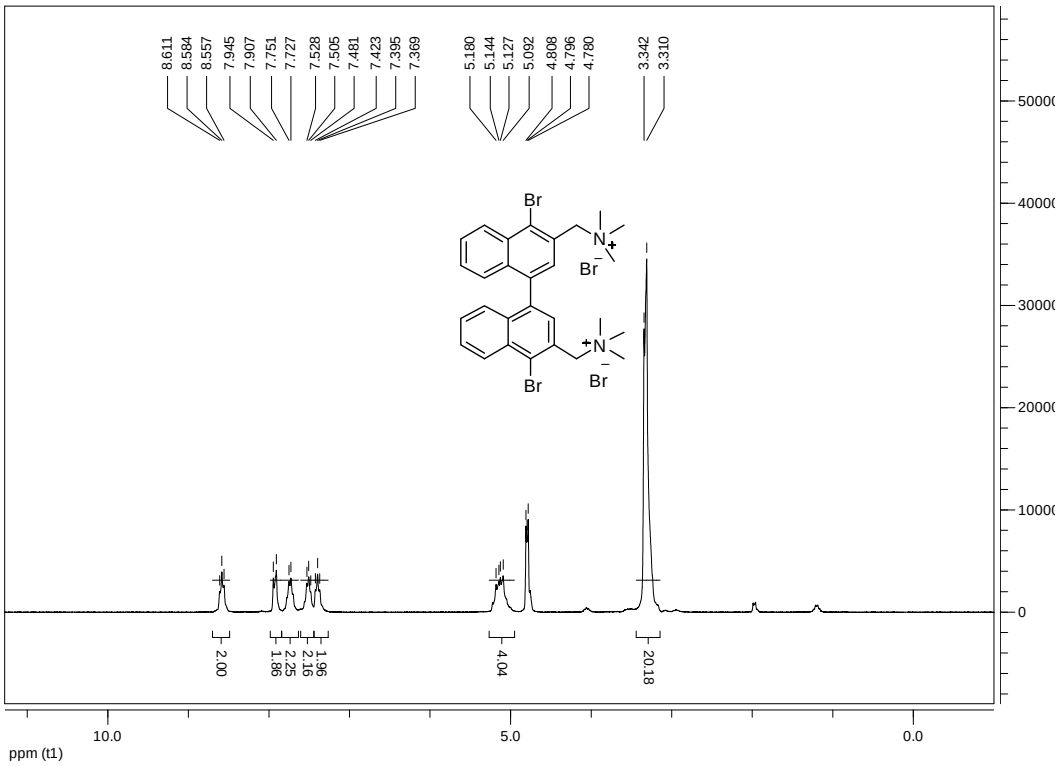

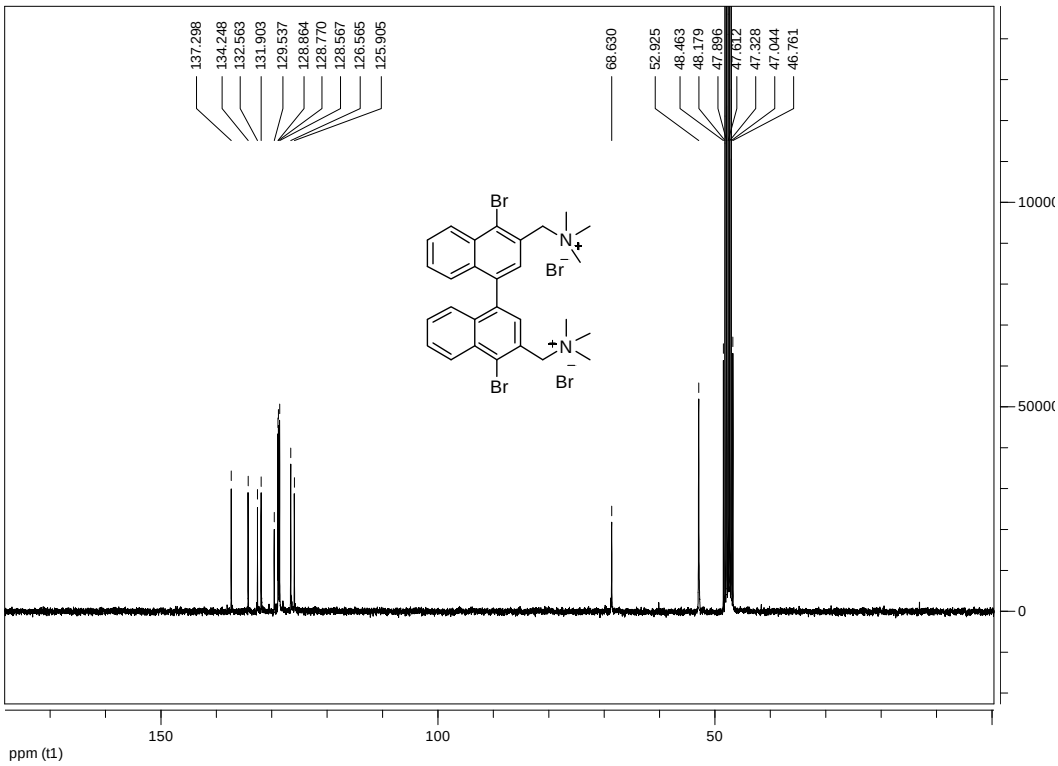

Figure S51. NMR of **3b**

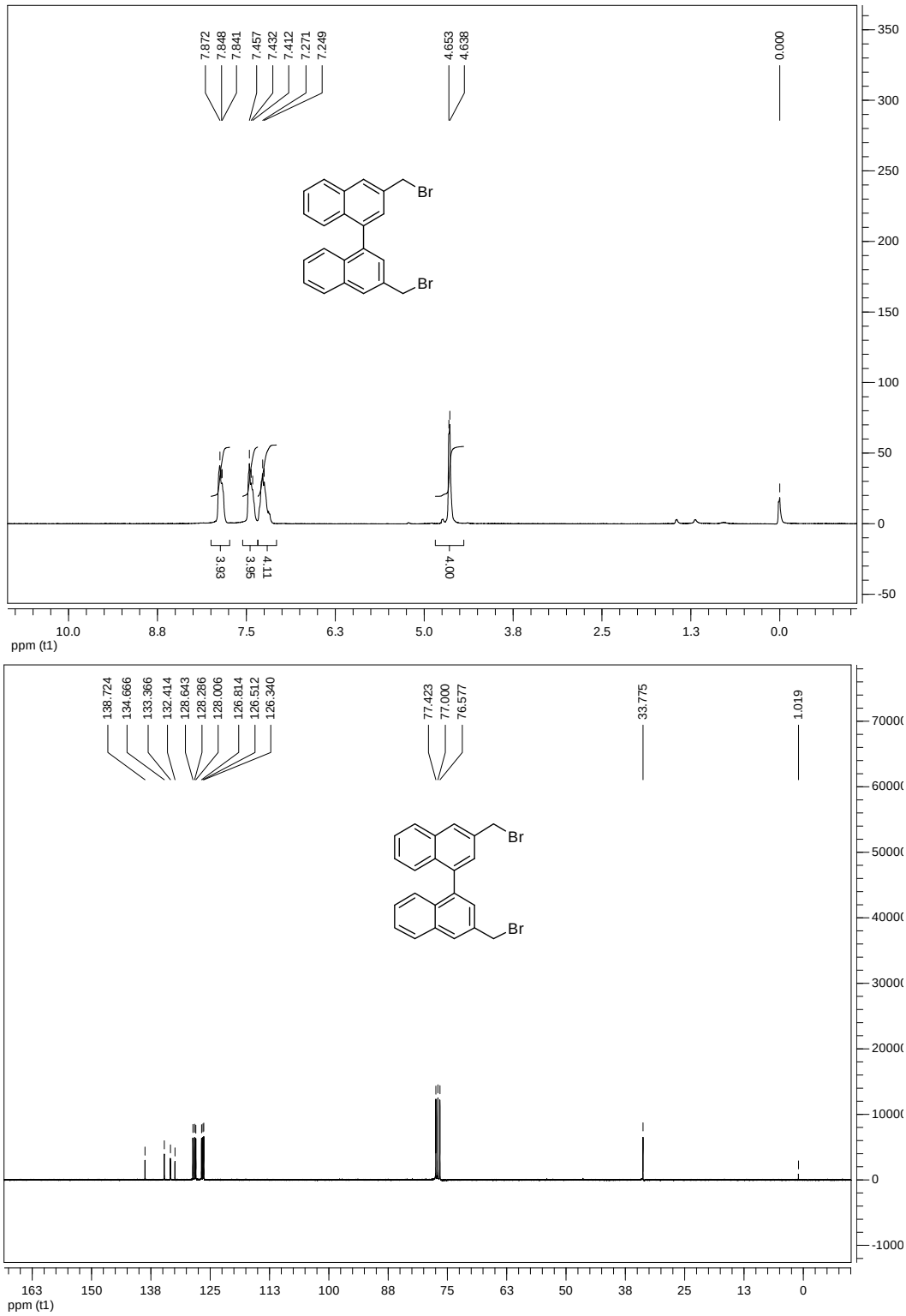

Figure S52. NMR of **2c**

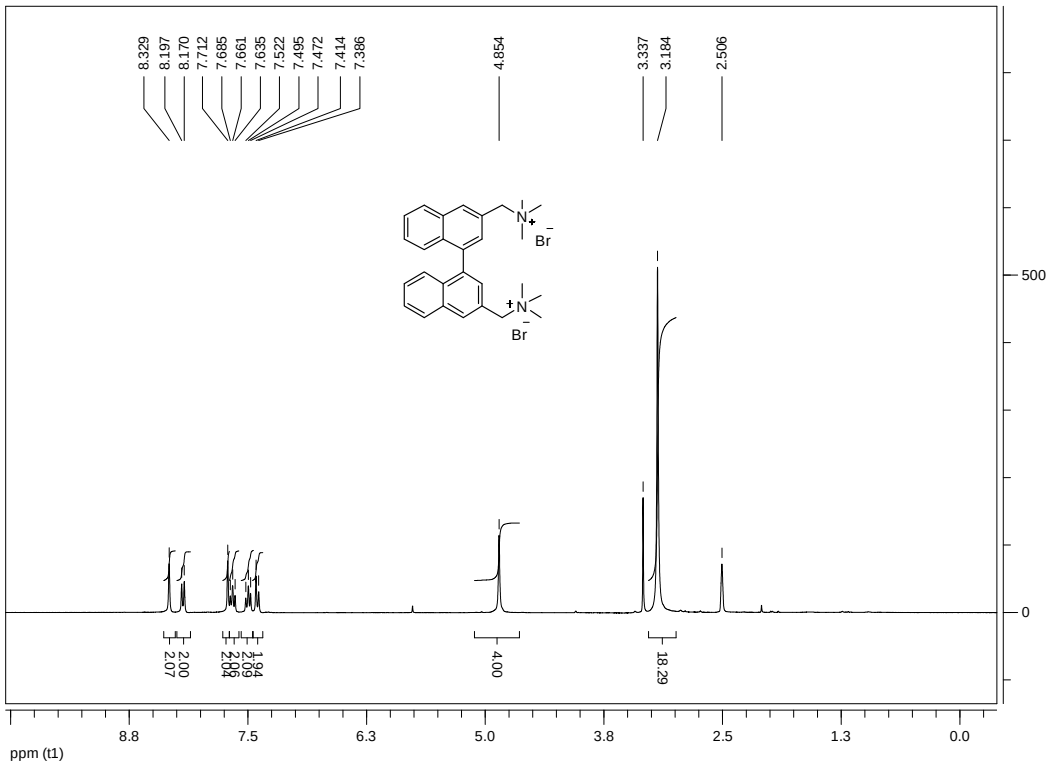

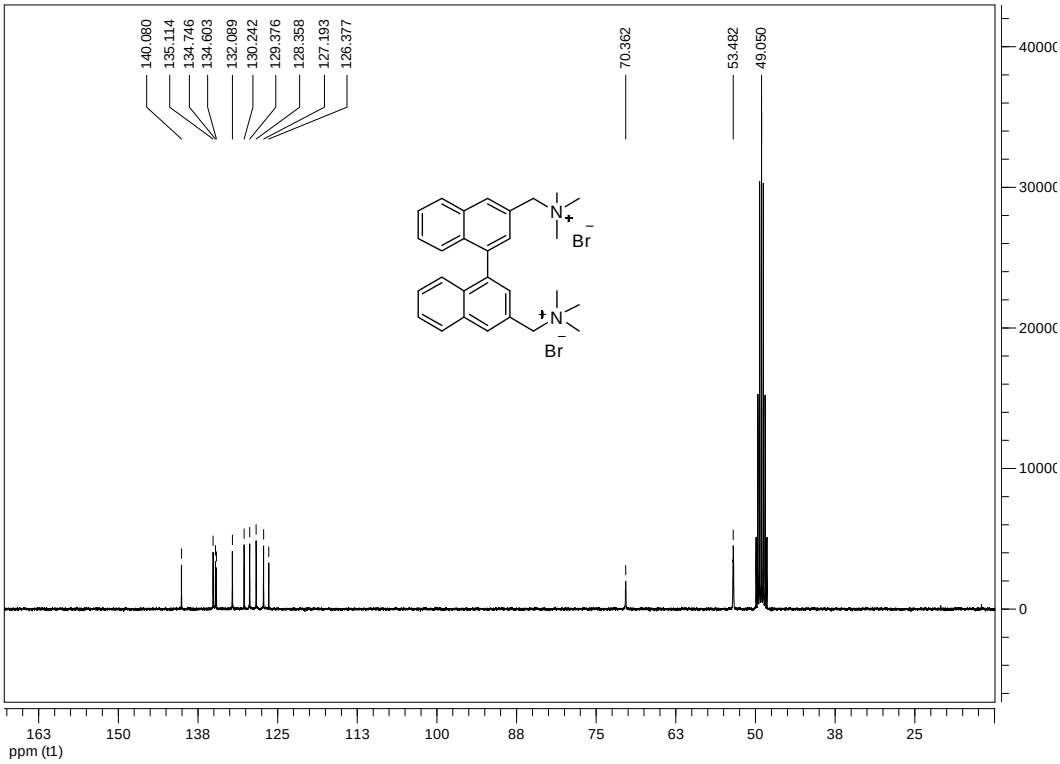

Figure S53. NMR of **3c**

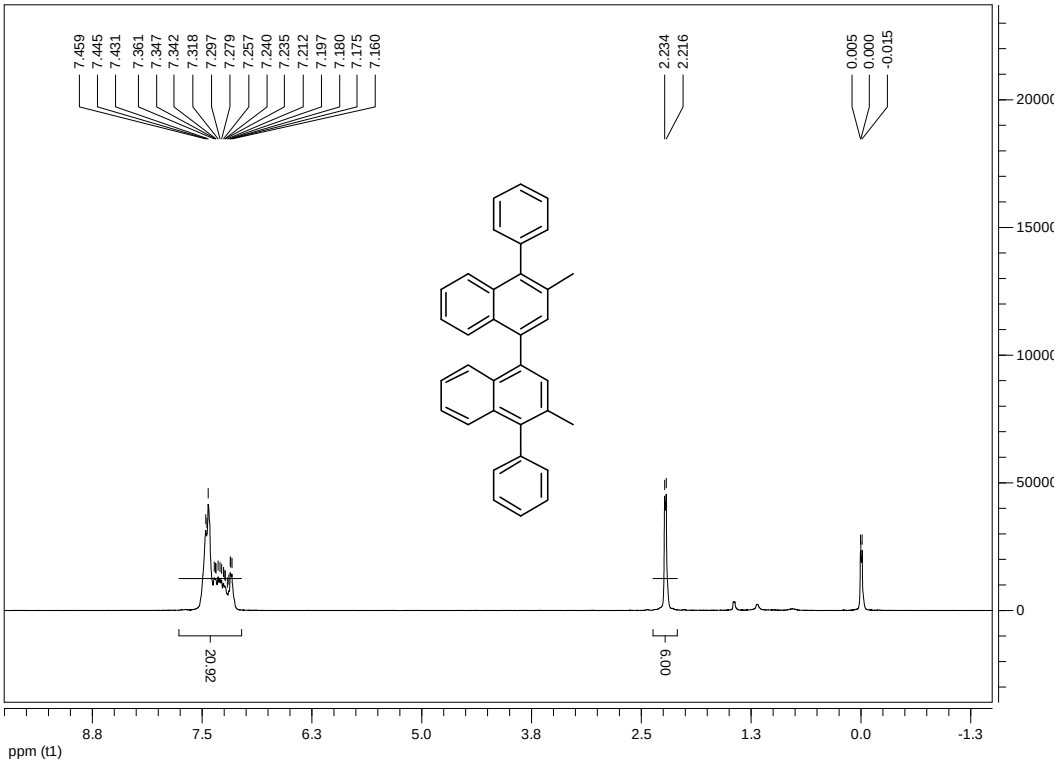

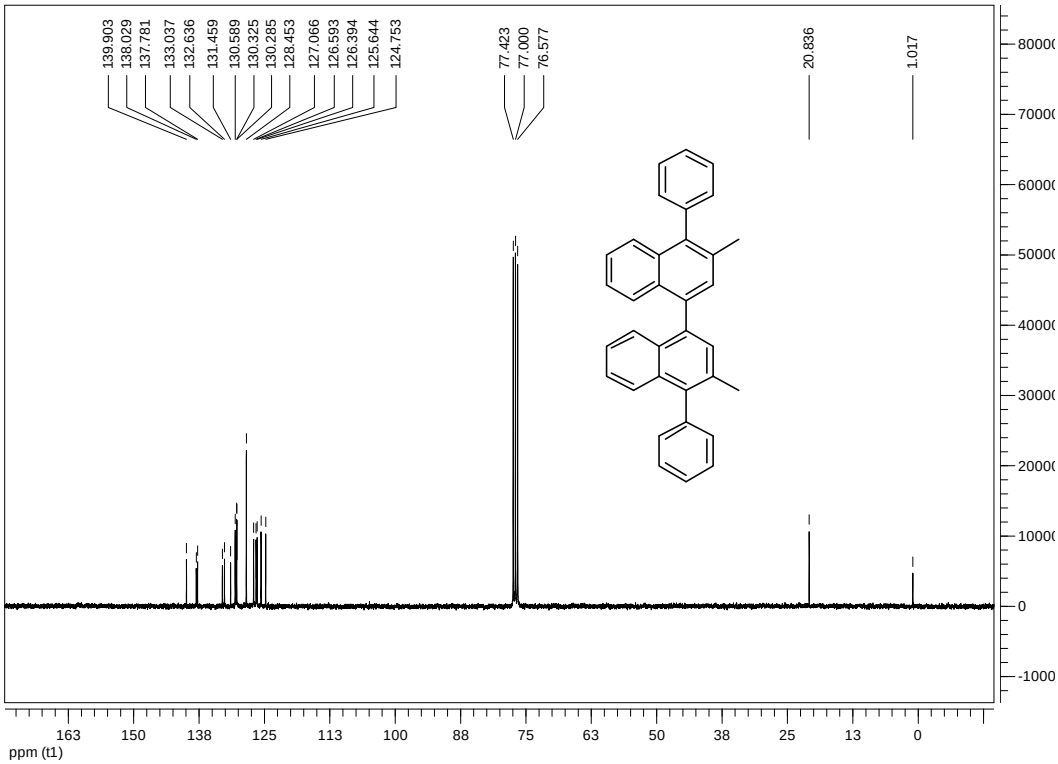

Figure S54. NMR of **12**

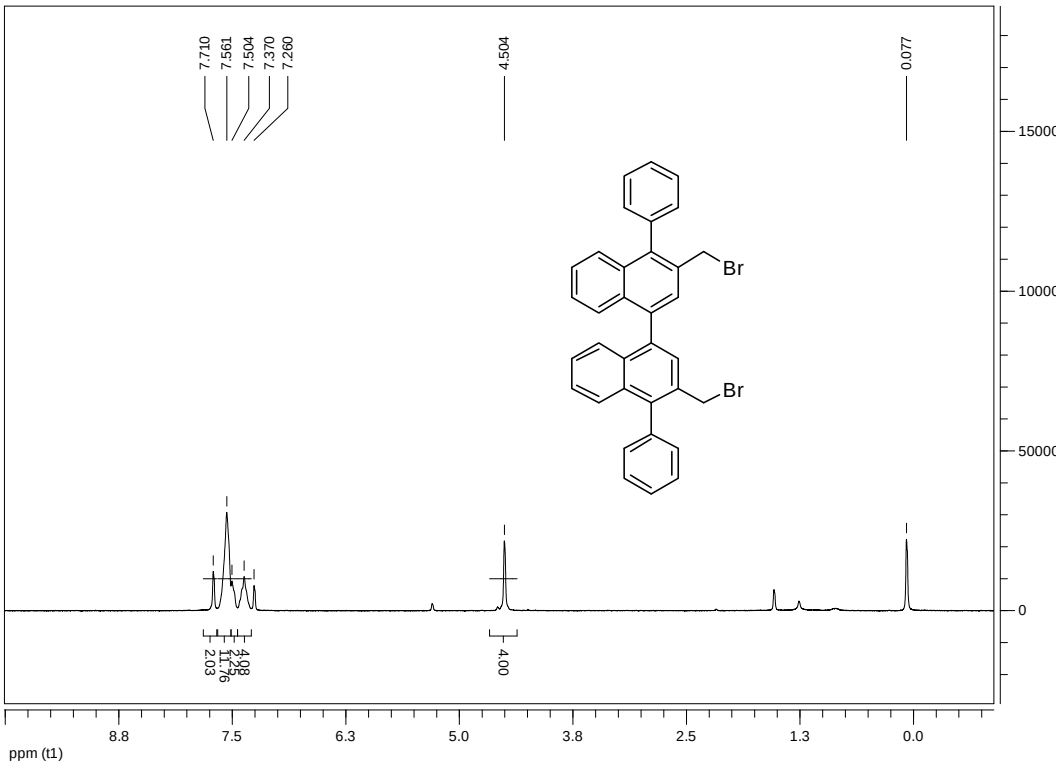

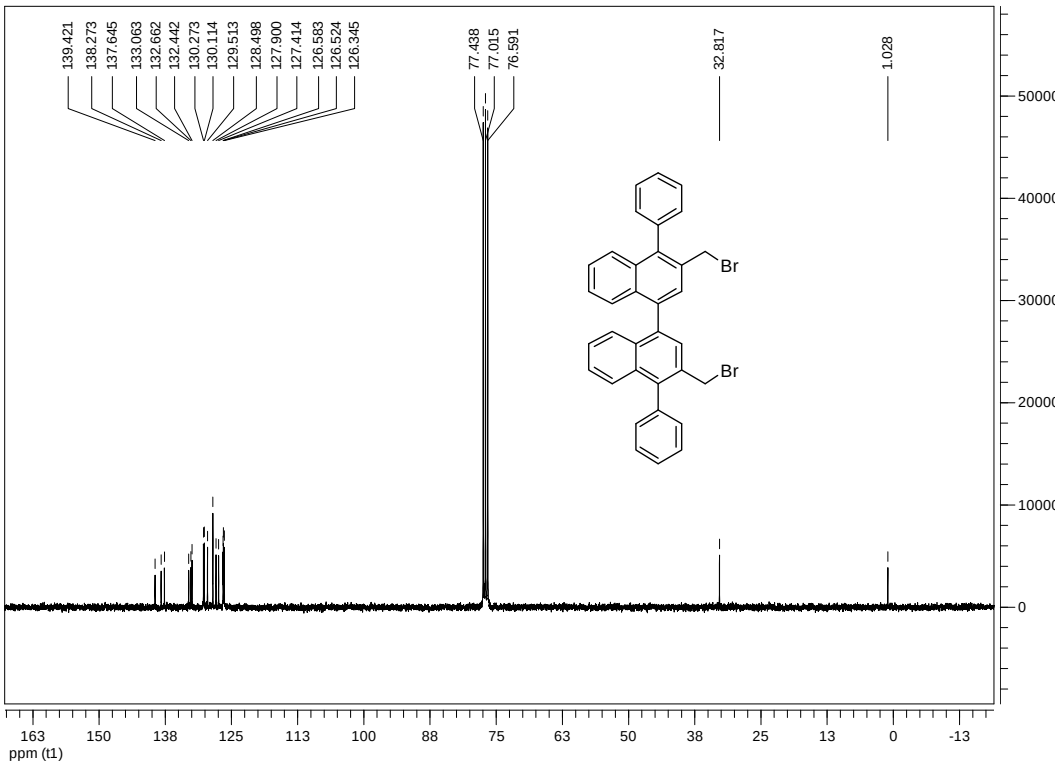

Figure S55. NMR of **2d**

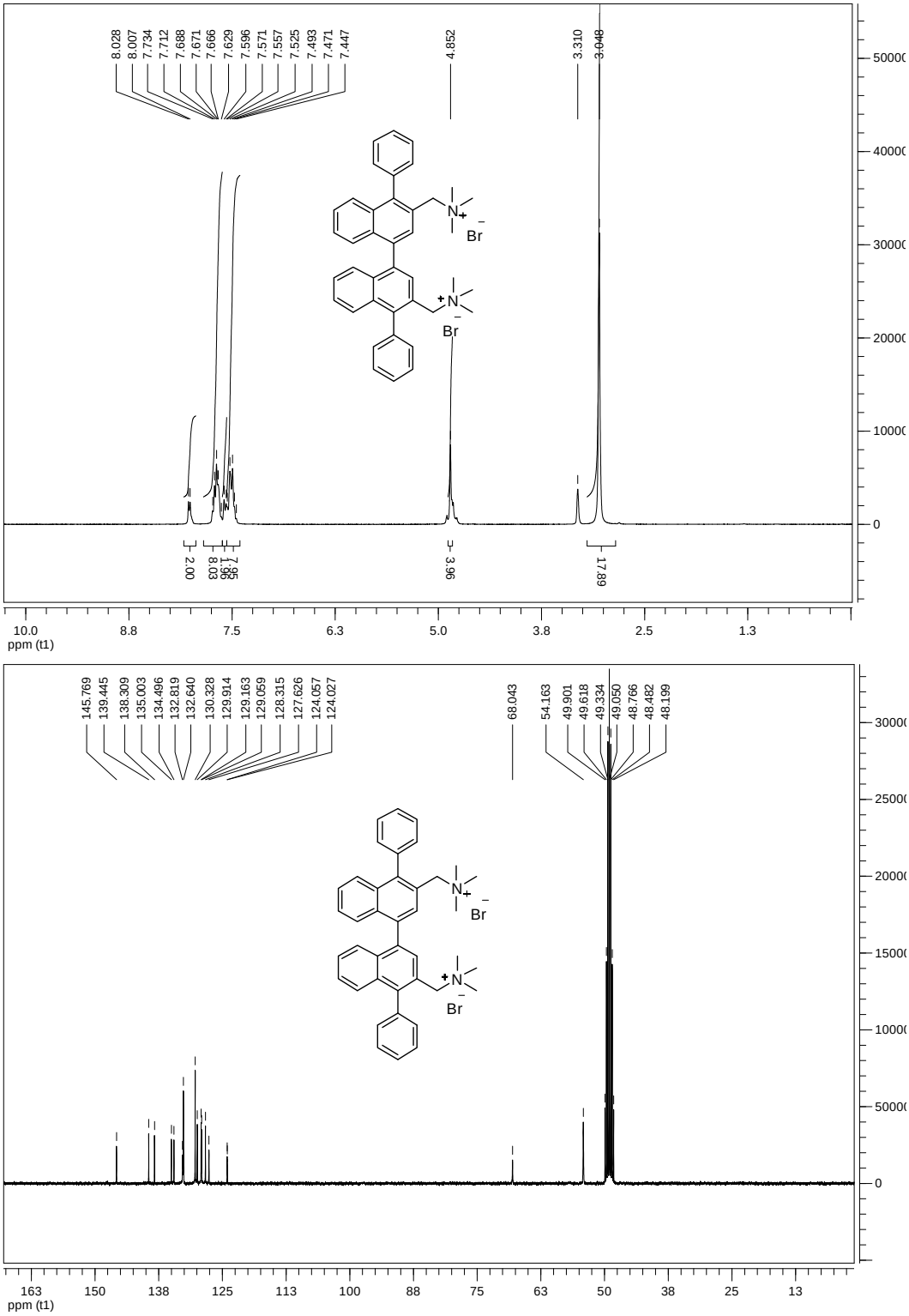

Figure S56. NMR of **3d**

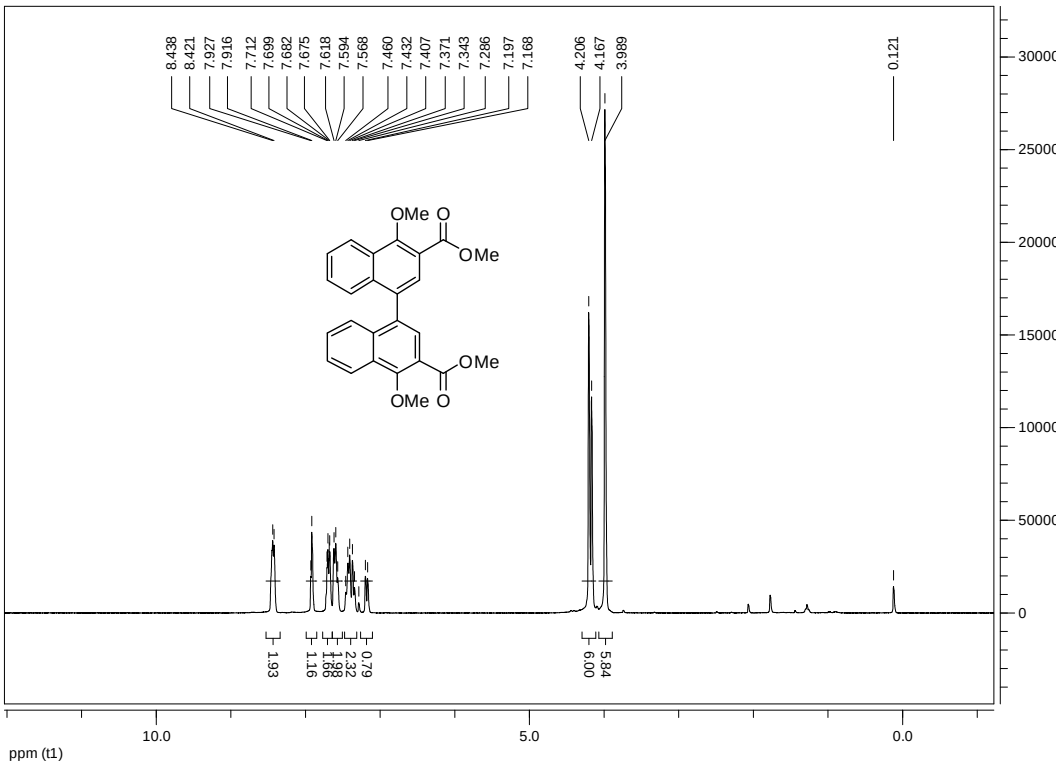

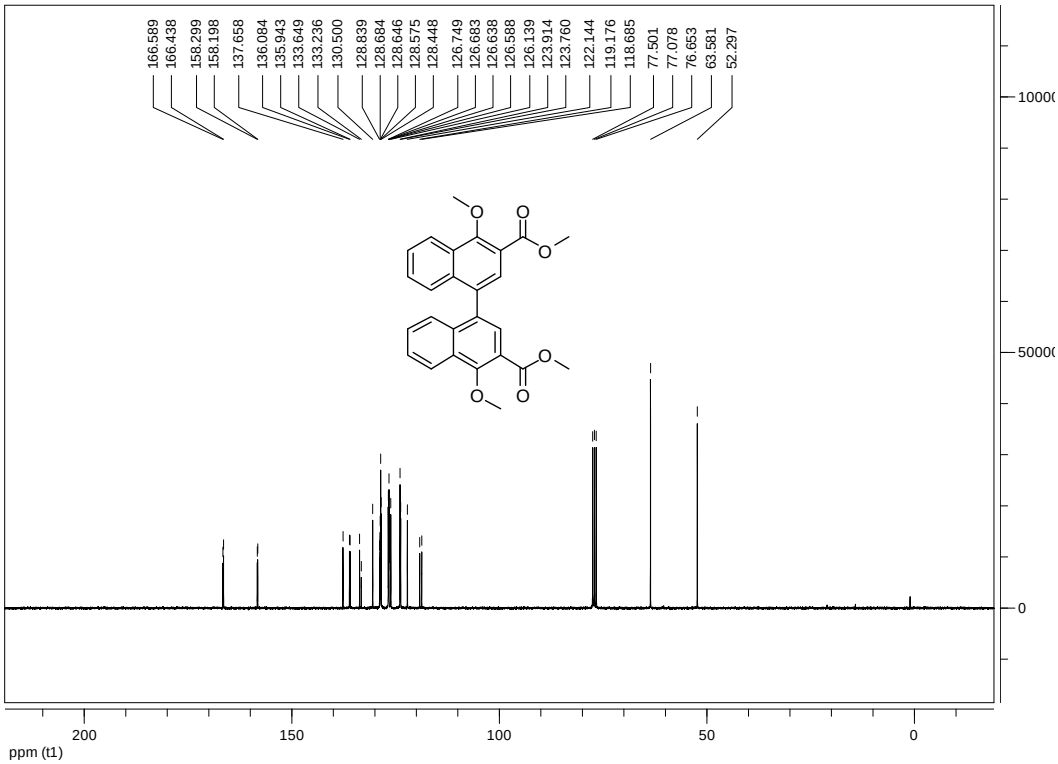

Figure S57. NMR of **8**

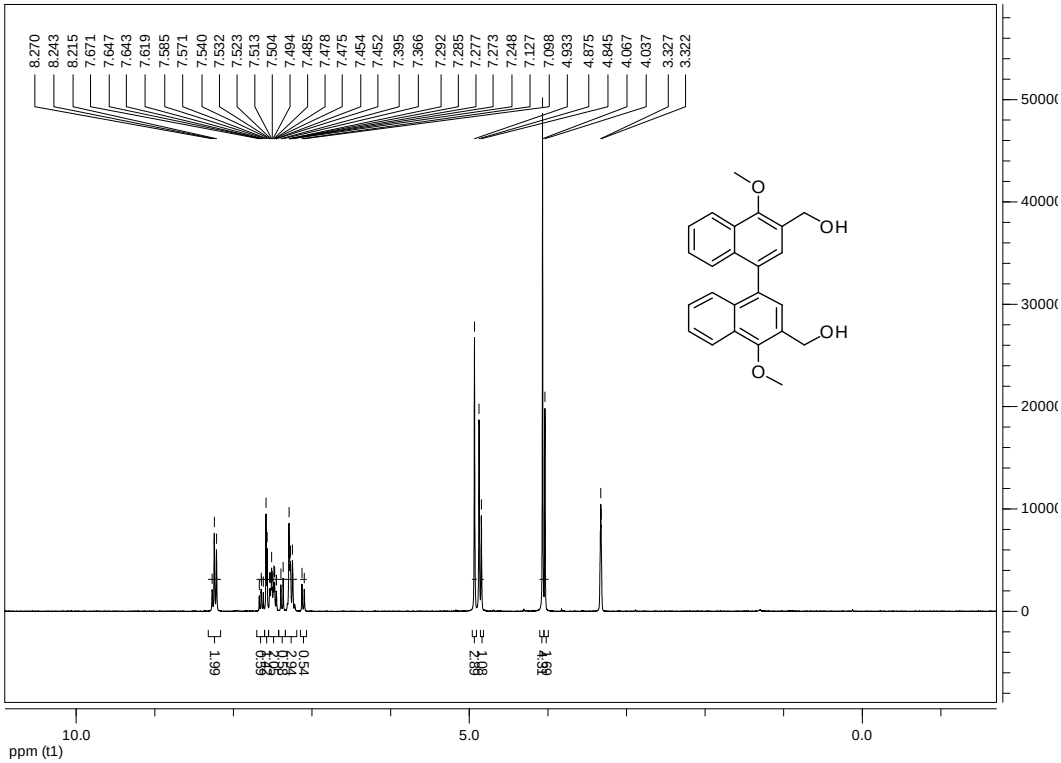

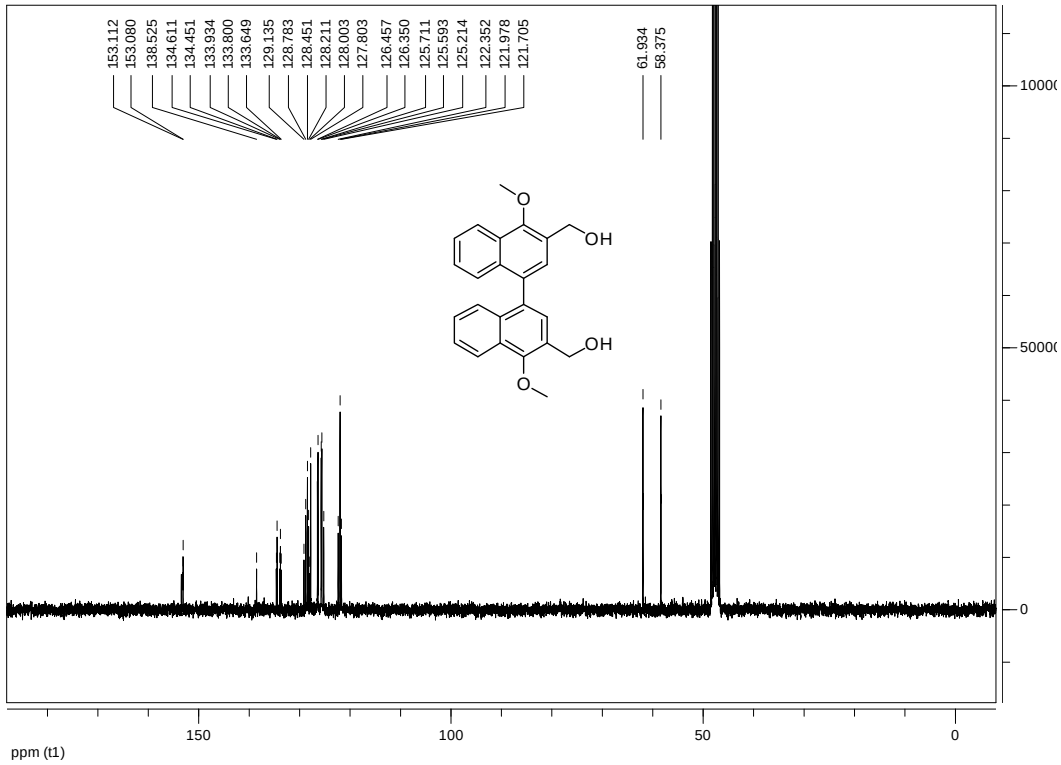

Figure S58. NMR of **9**

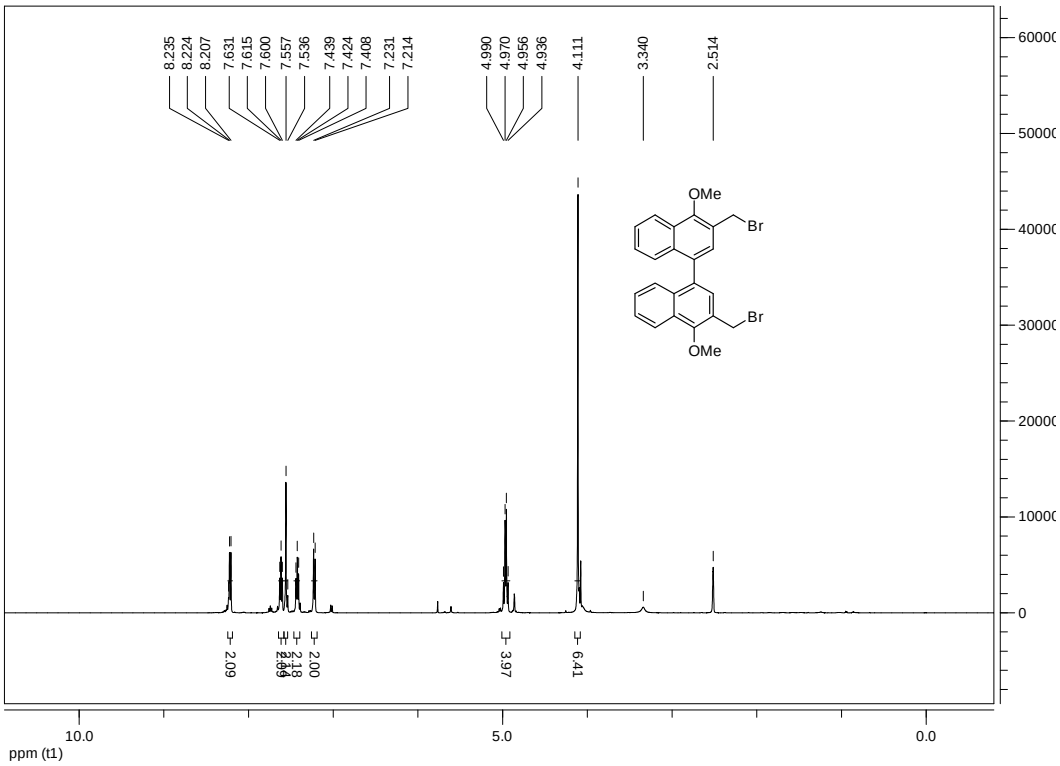

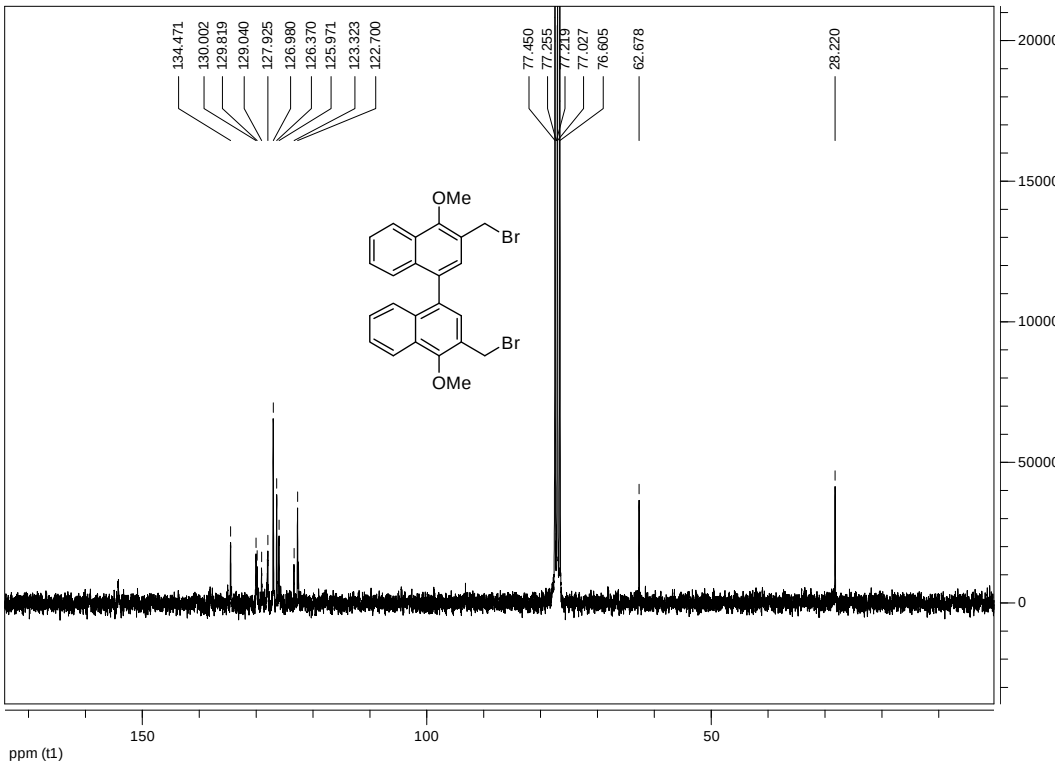

Figure S59. INMR of **2e**

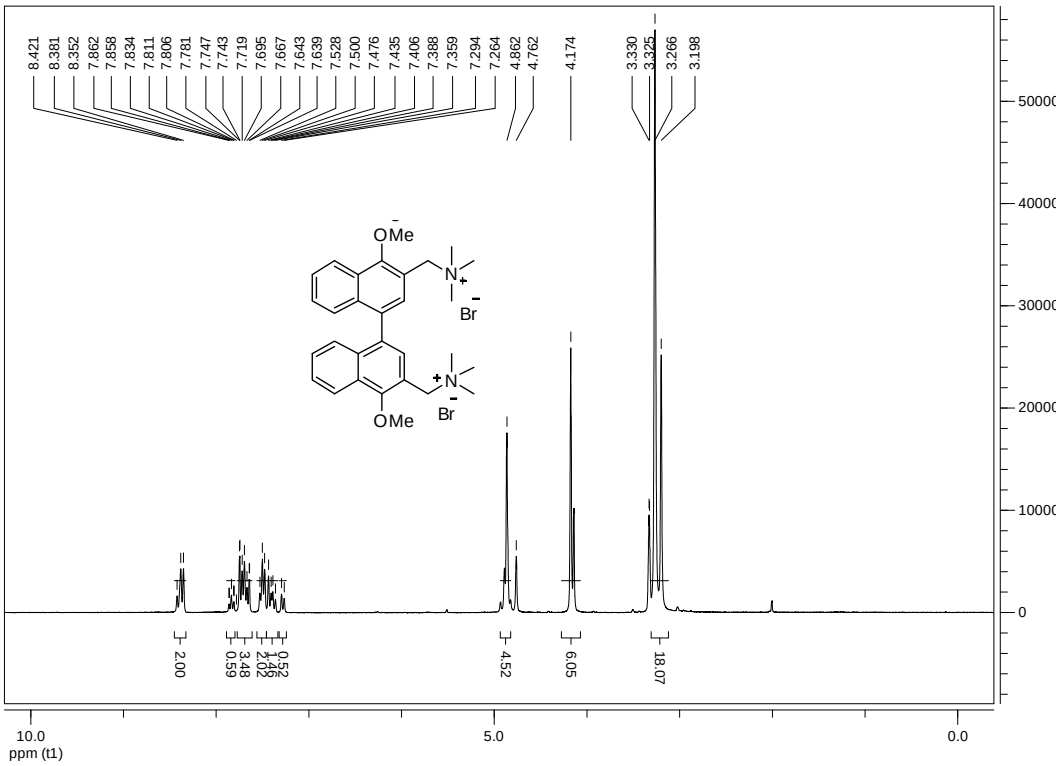

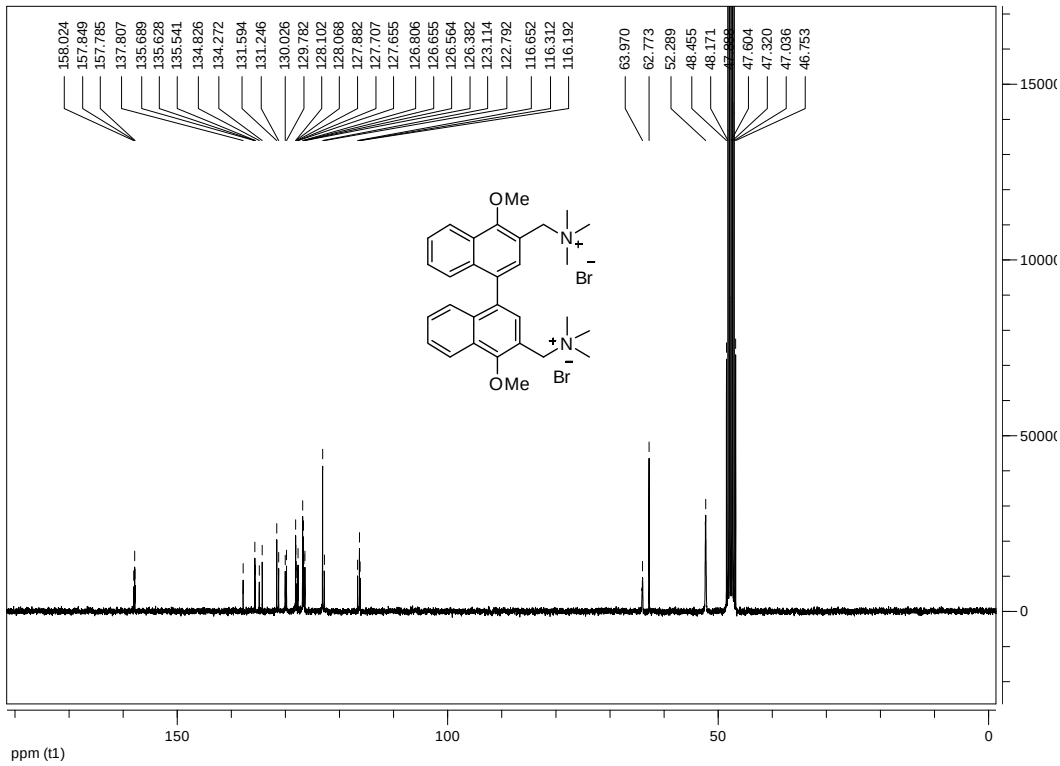

Figure S60. IT–TOF–MS(ESI) of **3e**

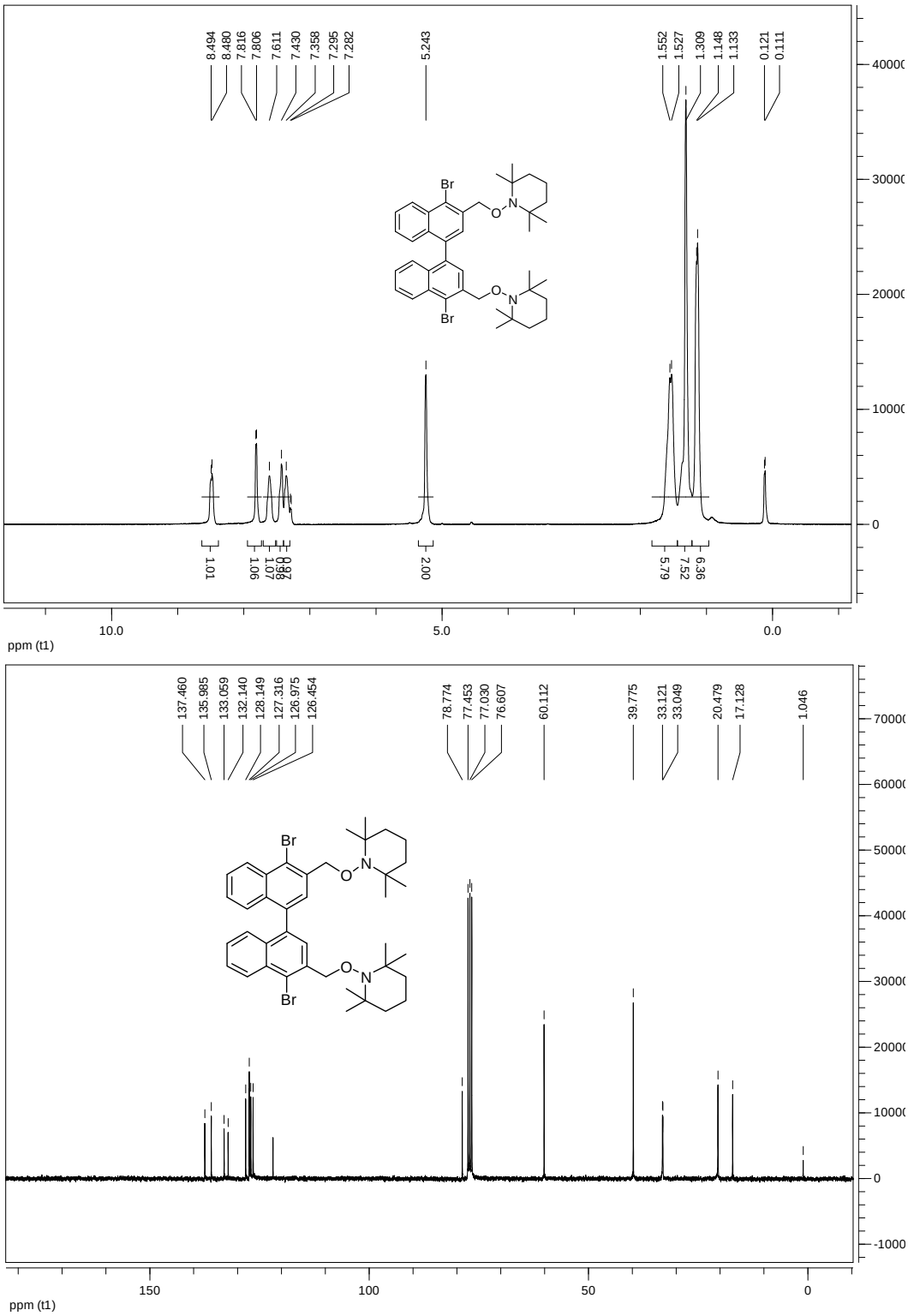

Figure S61. NMR of **18**

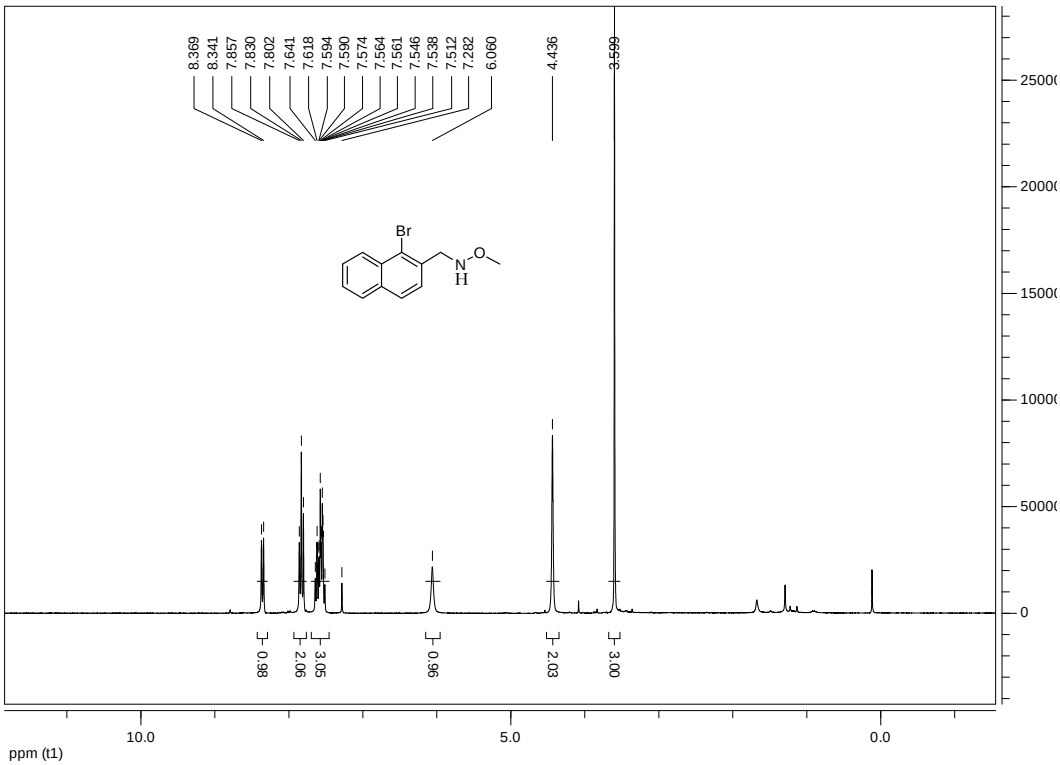

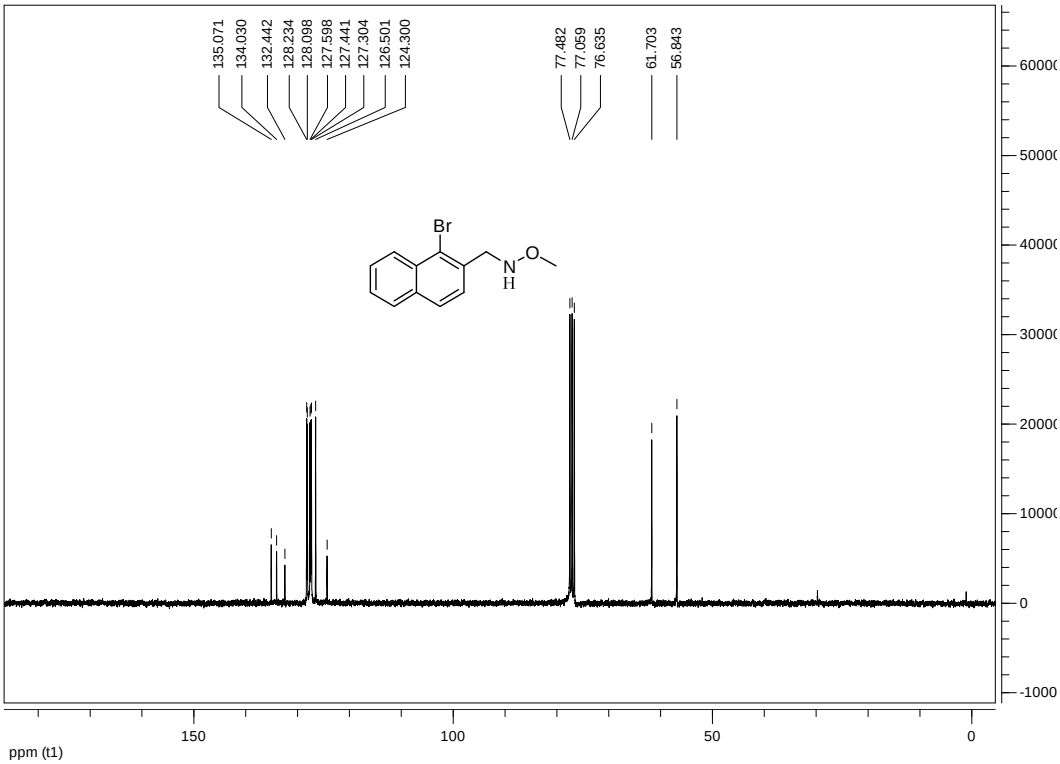

Figure S62. NMR of **23**

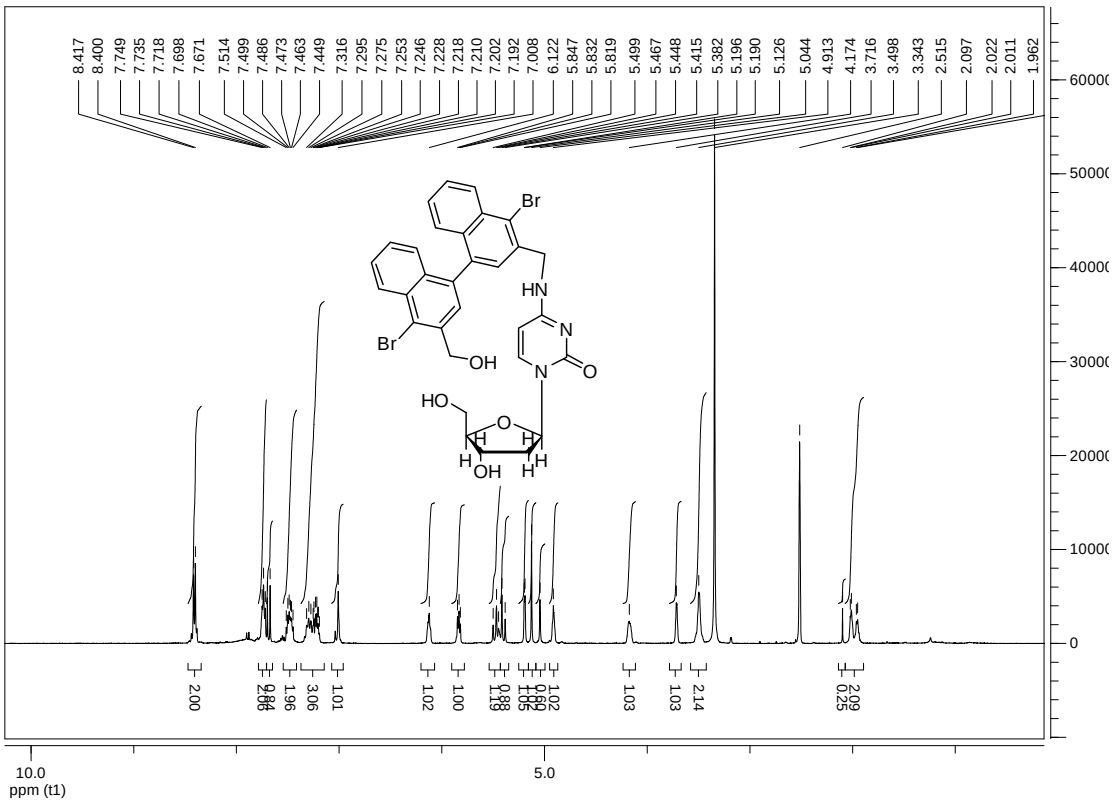

Figure S63. NMR of **24**

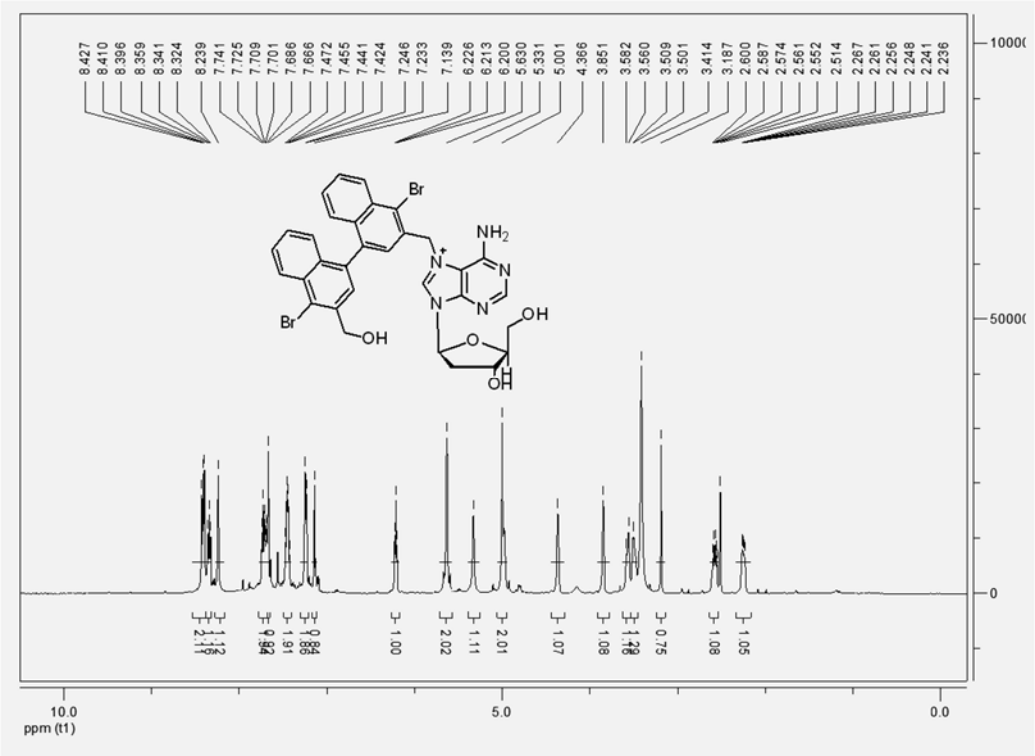

Figure S64. NMR of **25a**

9. Mass spectra of new compounds

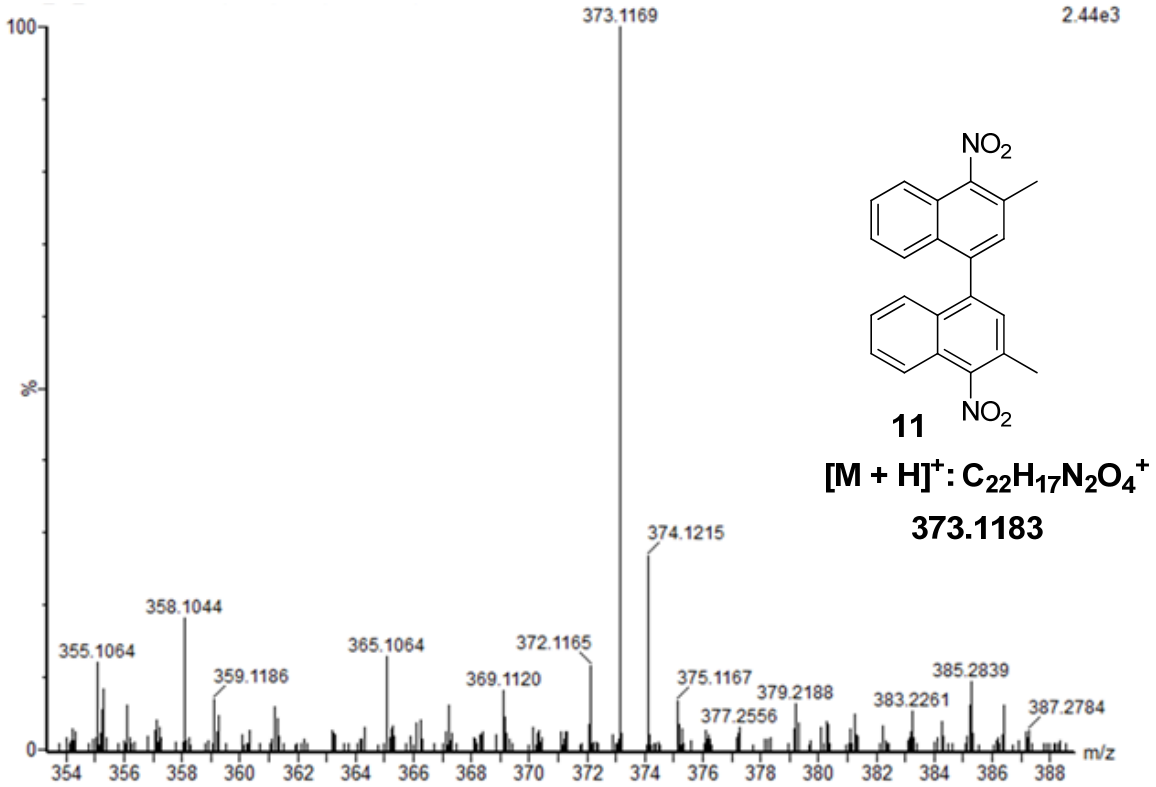

Figure S65. IT–TOF–MS (ESI) of **11**

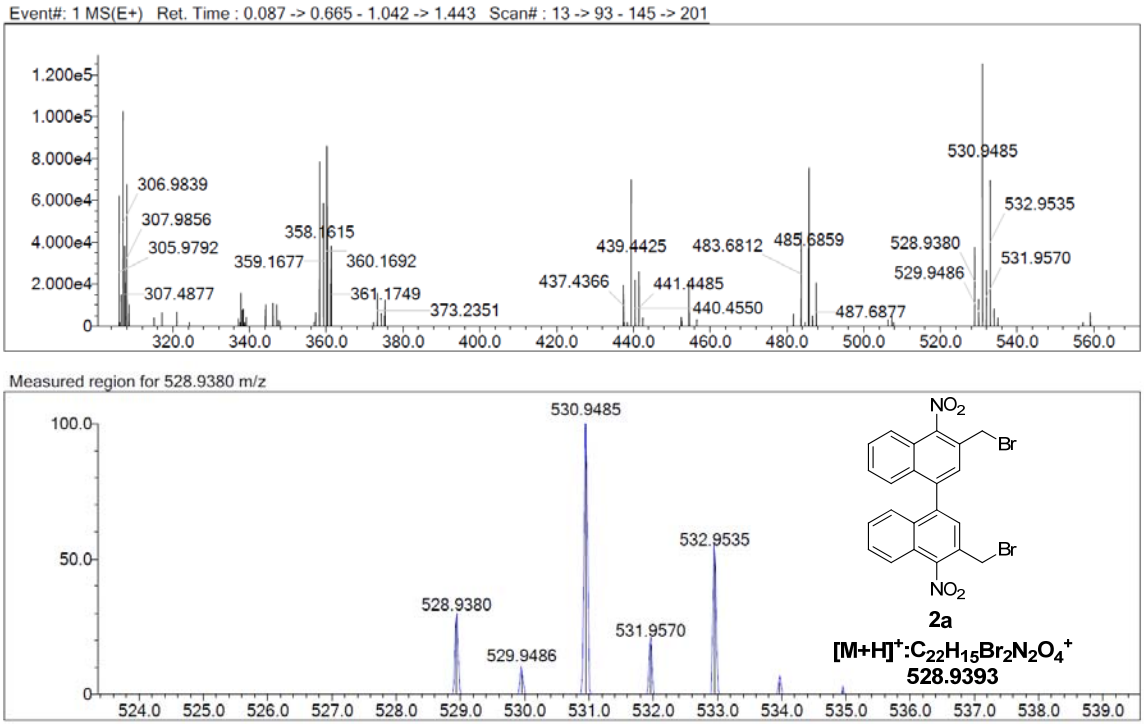

Figure S66. IT–TOF–MS (ESI) of **2a.**

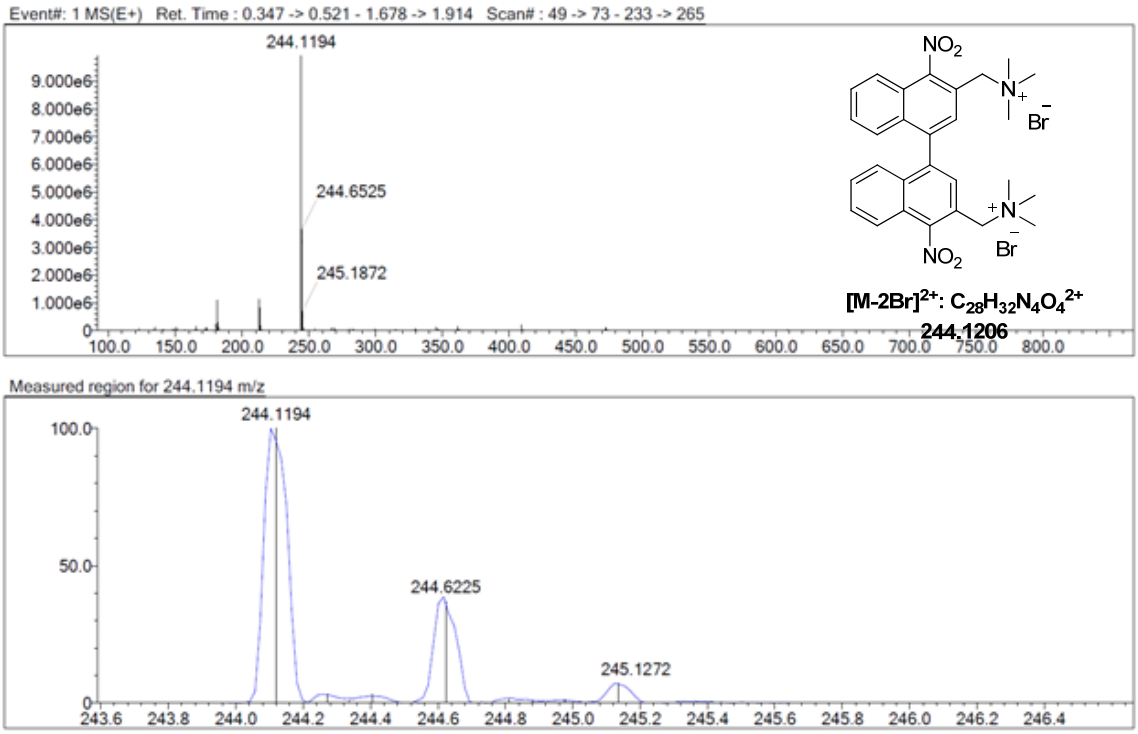

Figure S67. IT–TOF–MS (ESI) of **3a.**

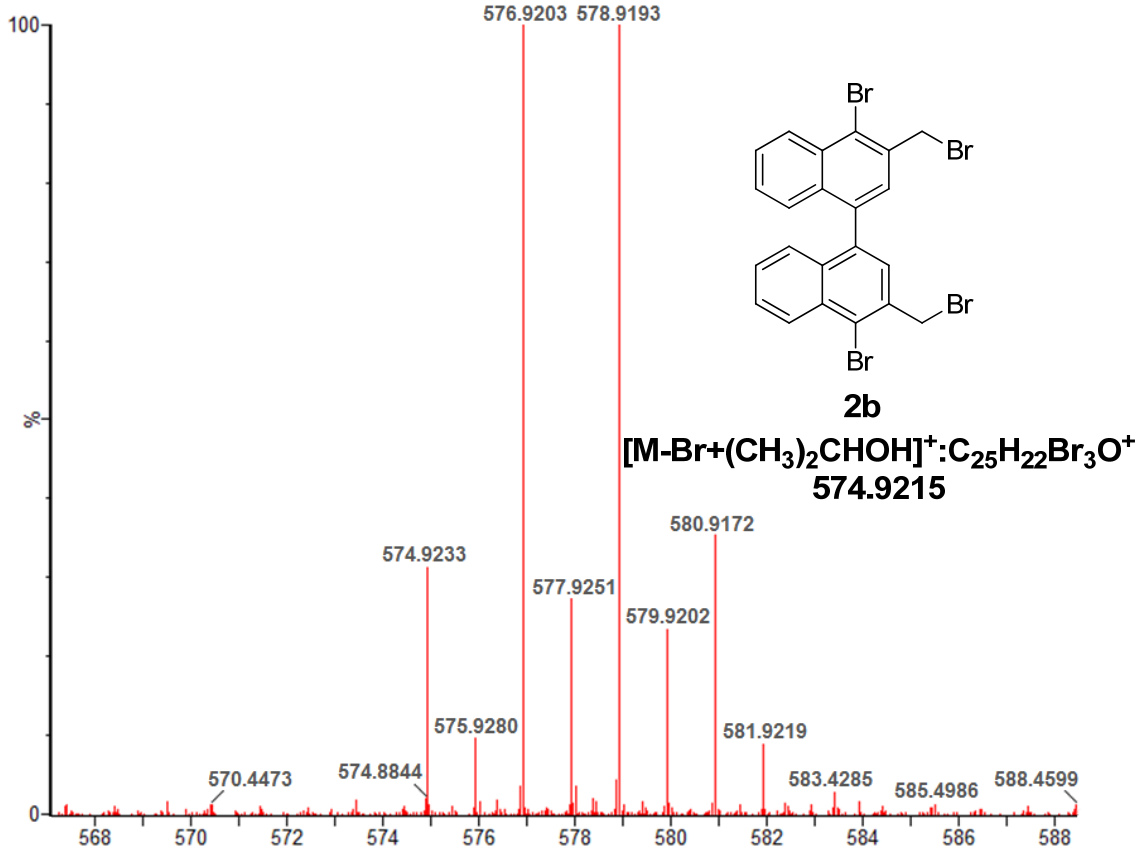

Figure S68. IT–TOF–MS (ESI) of **2b.**

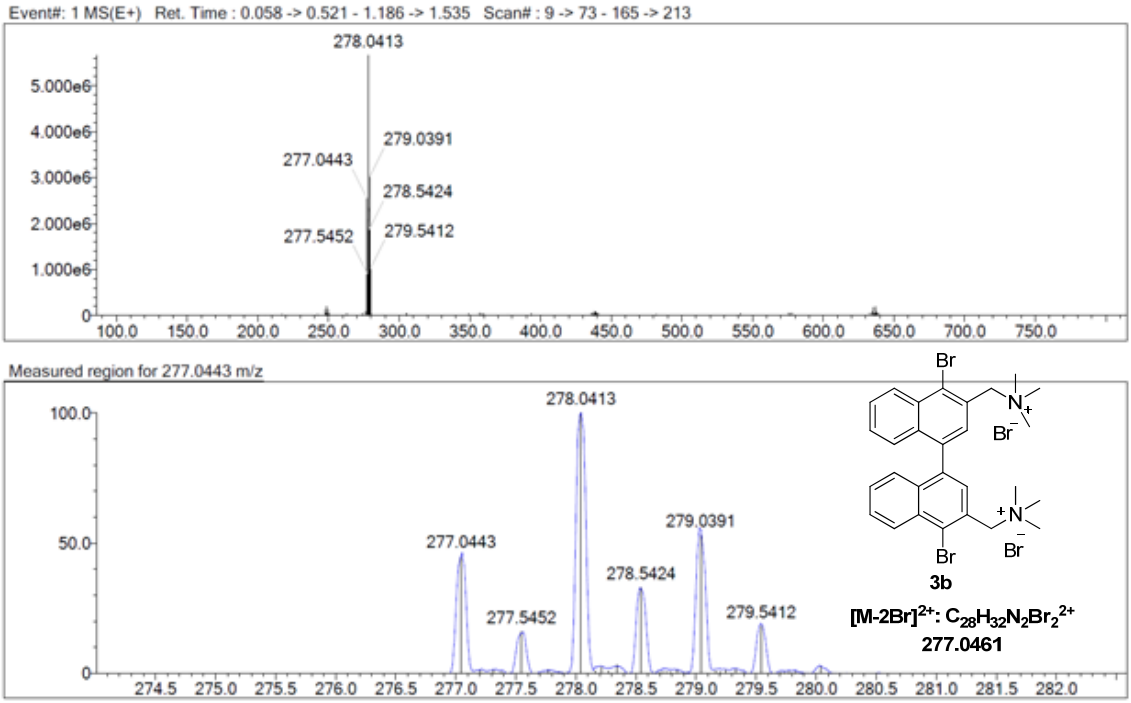

Figure S69. IT–TOF–MS (ESI) of **3b.**

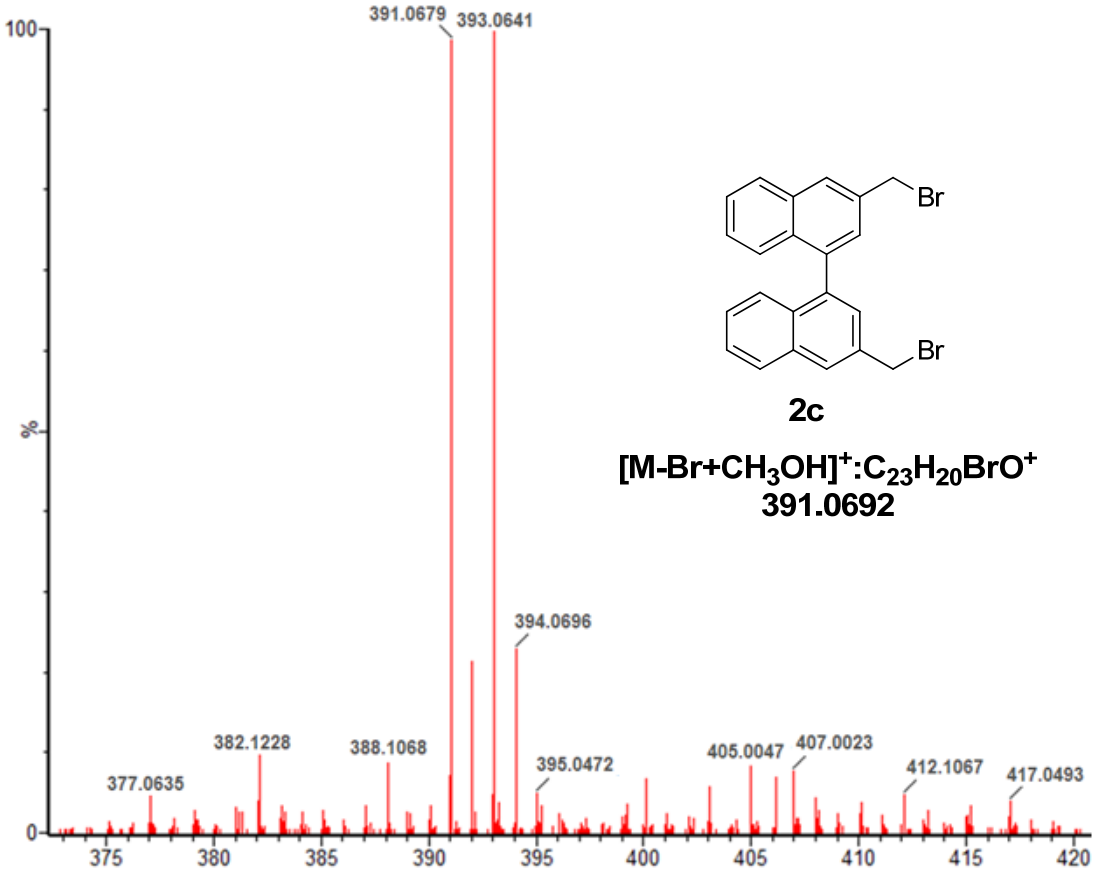

Figure S70. IT–TOF–MS (ESI) of **2c.**

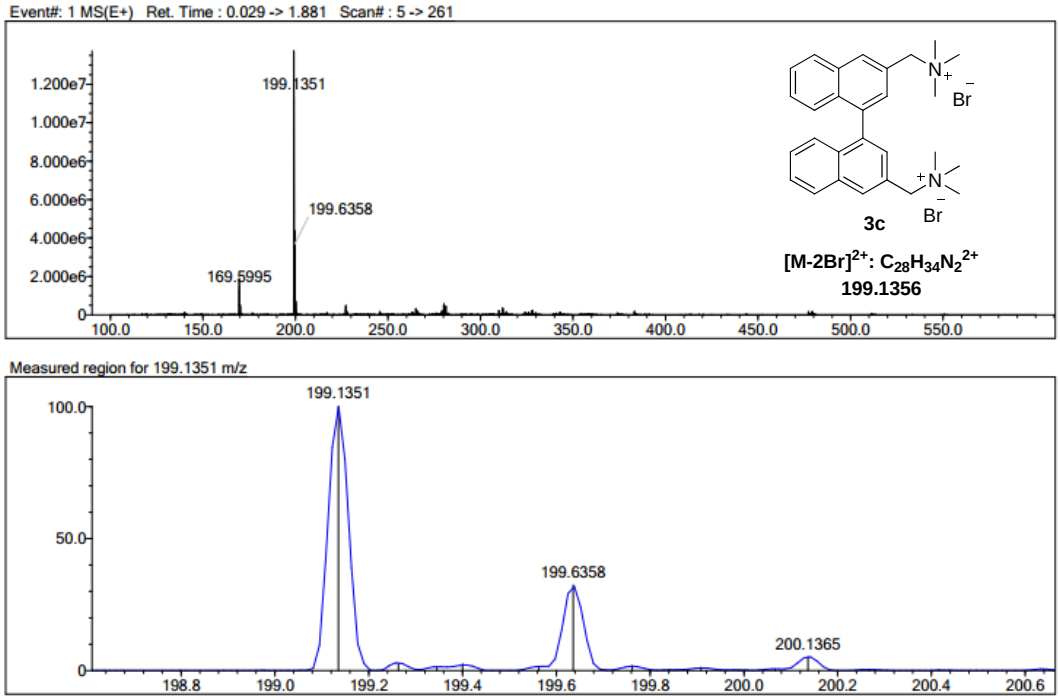

Figure S71. IT–TOF–MS (ESI) of **3c.**

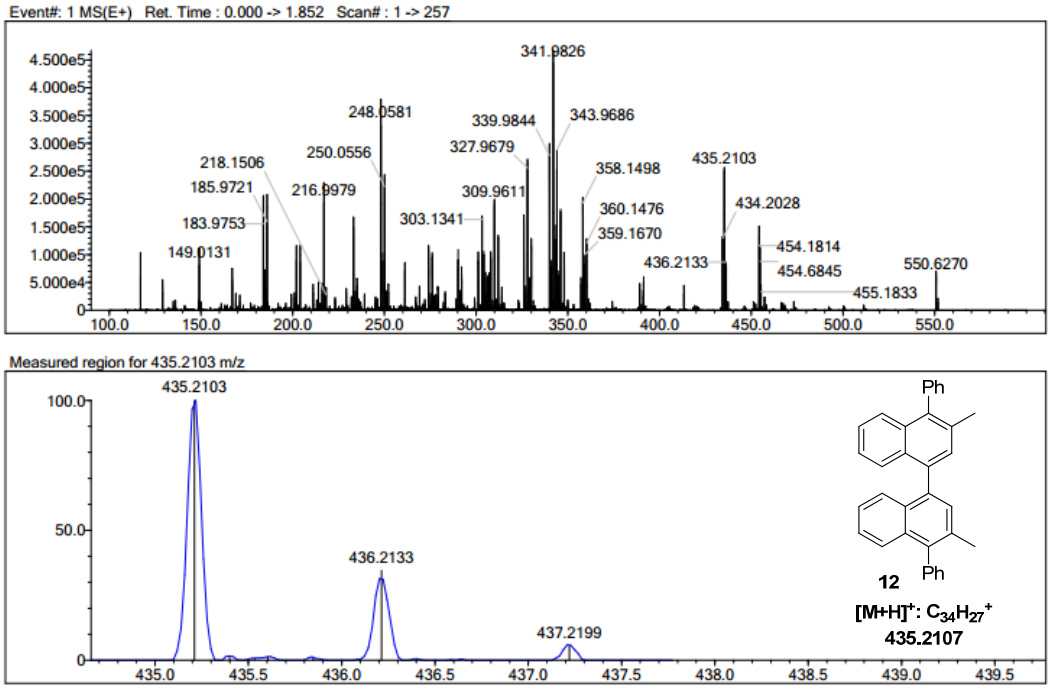

Figure S72. IT–TOF–MS (ESI) of **12.**

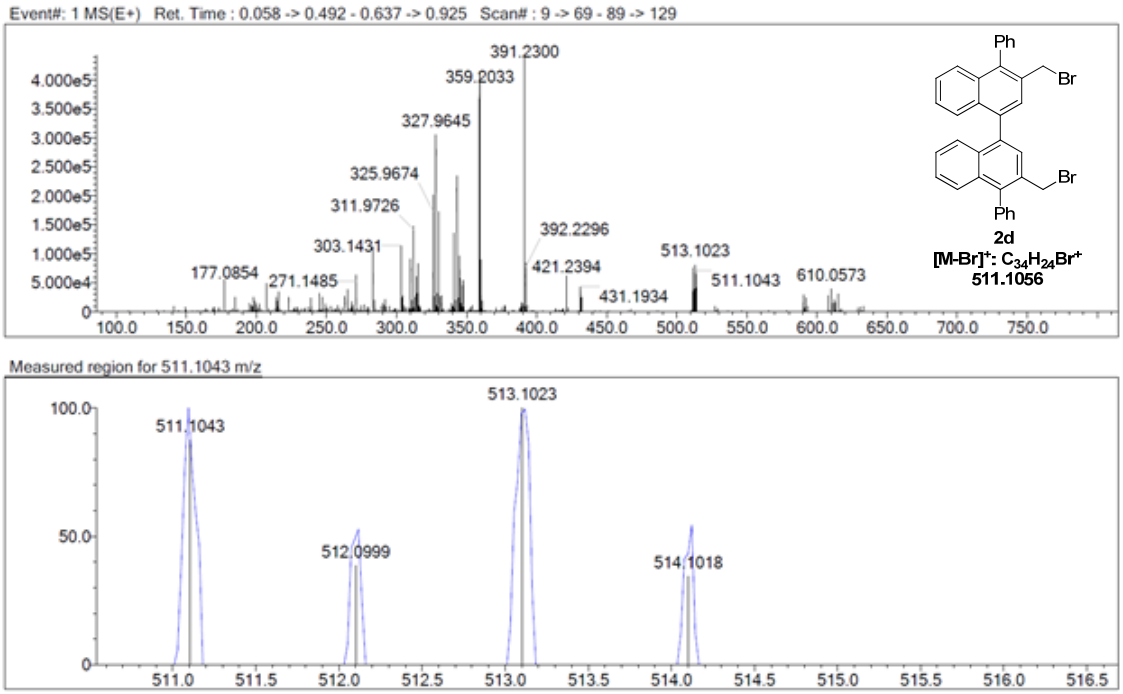

Figure S73. IT–TOF–MS (ESI) of **2d.**

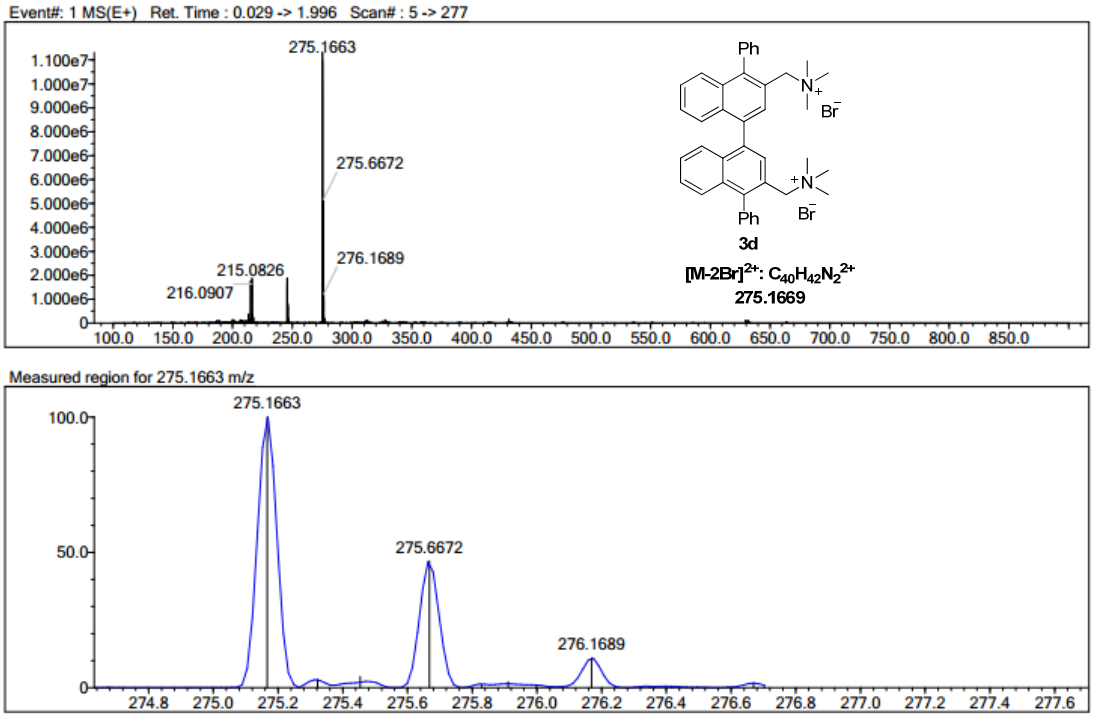

Figure S74. IT–TOF–MS (ESI) of **3d.**

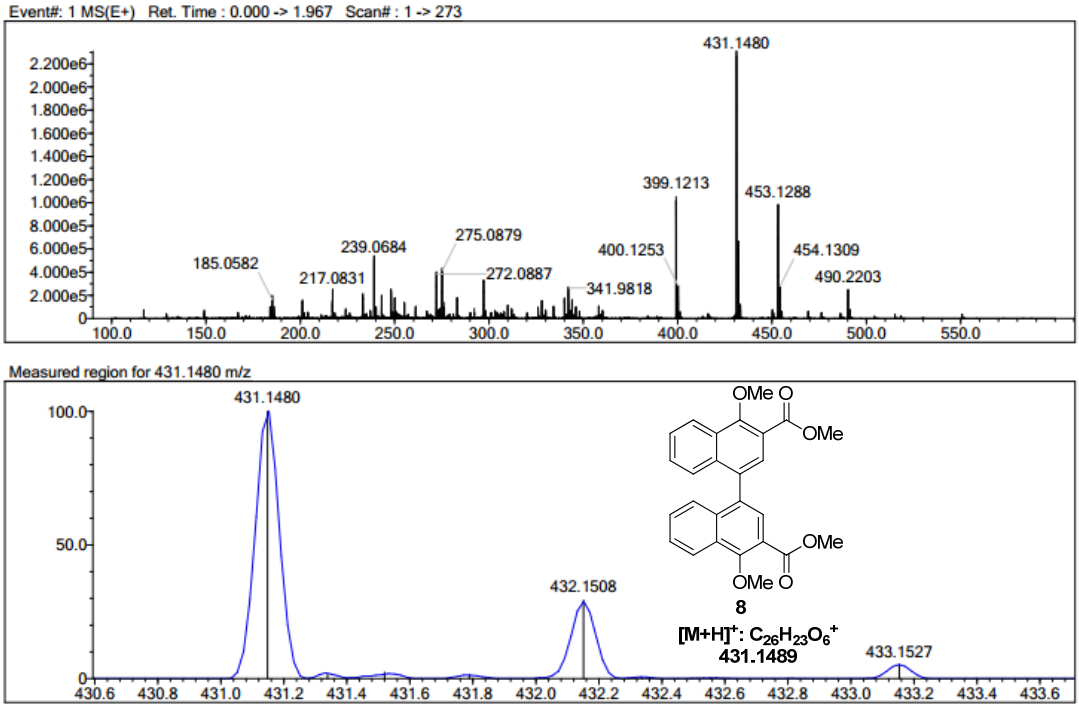

Figure S75. IT–TOF–MS (ESI) of **8.**

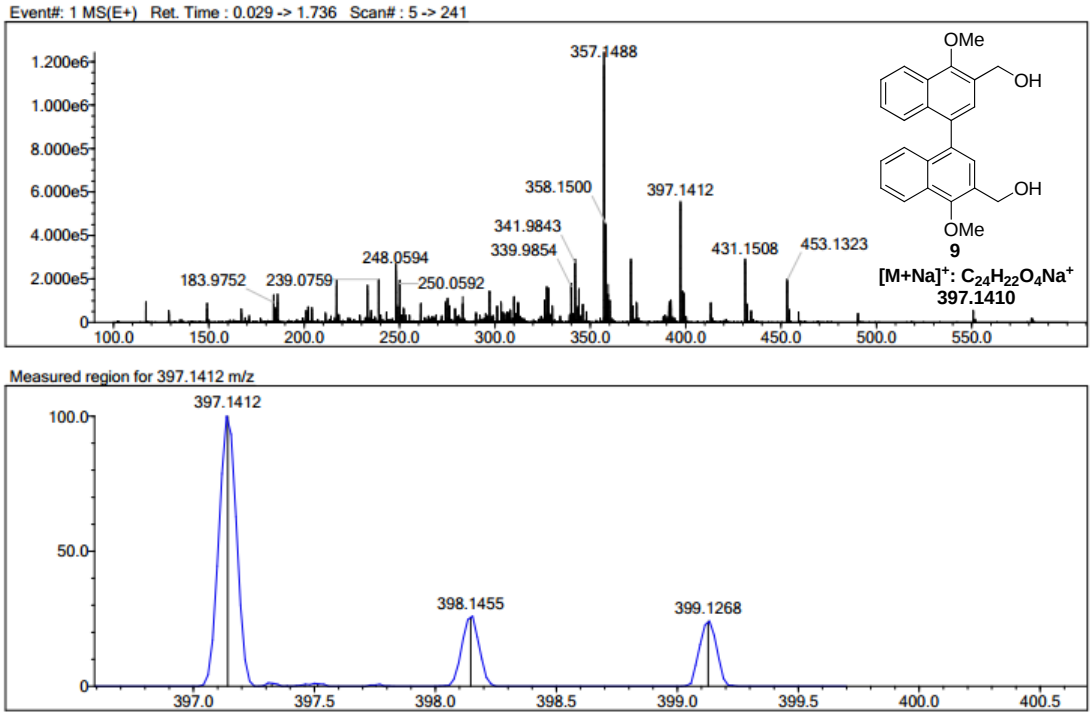

Figure S76. IT–TOF–MS (ESI) of **9.**

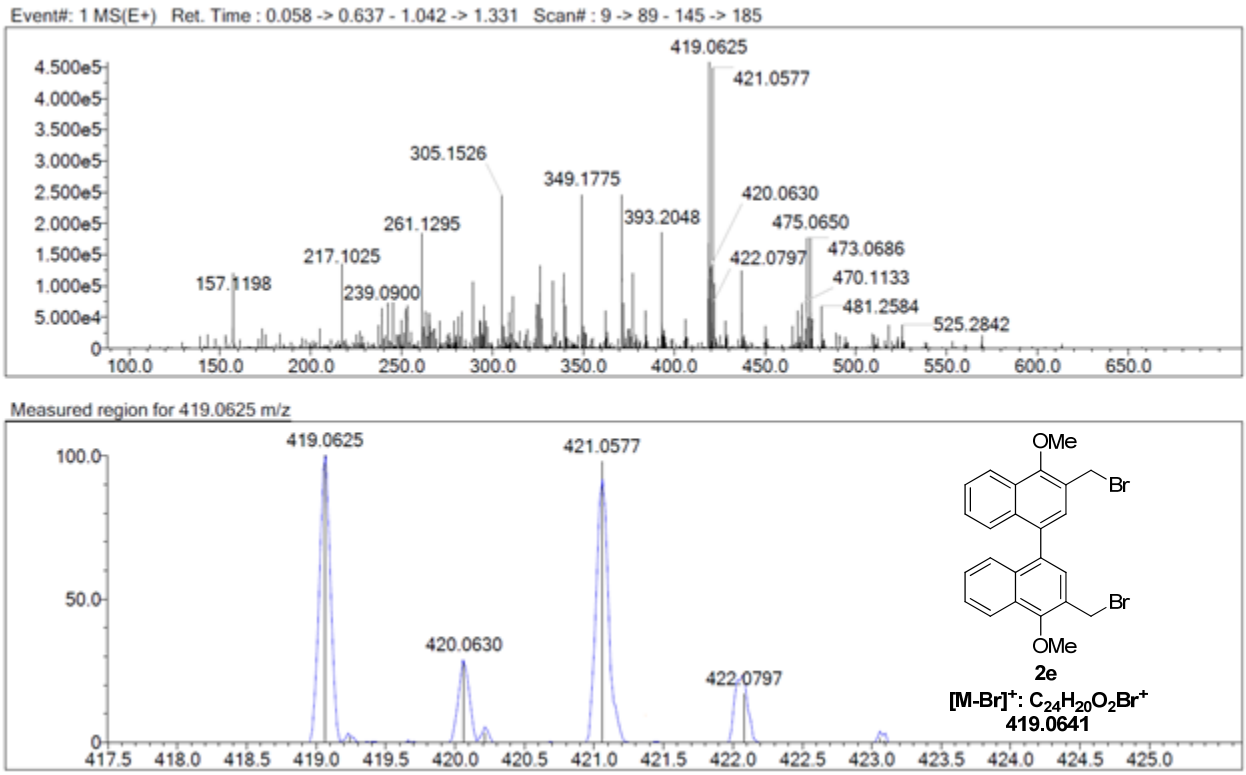

Figure S77. IT–TOF–MS (ESI) of **2e.**

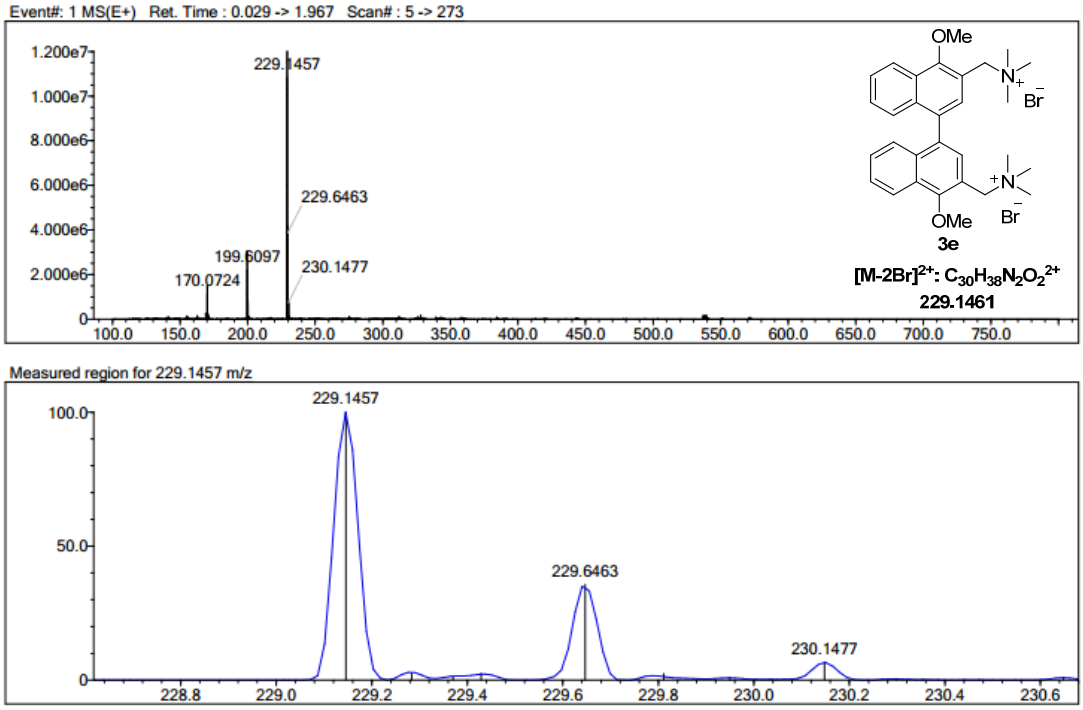

Figure S78. IT–TOF–MS (ESI) of **3e.**

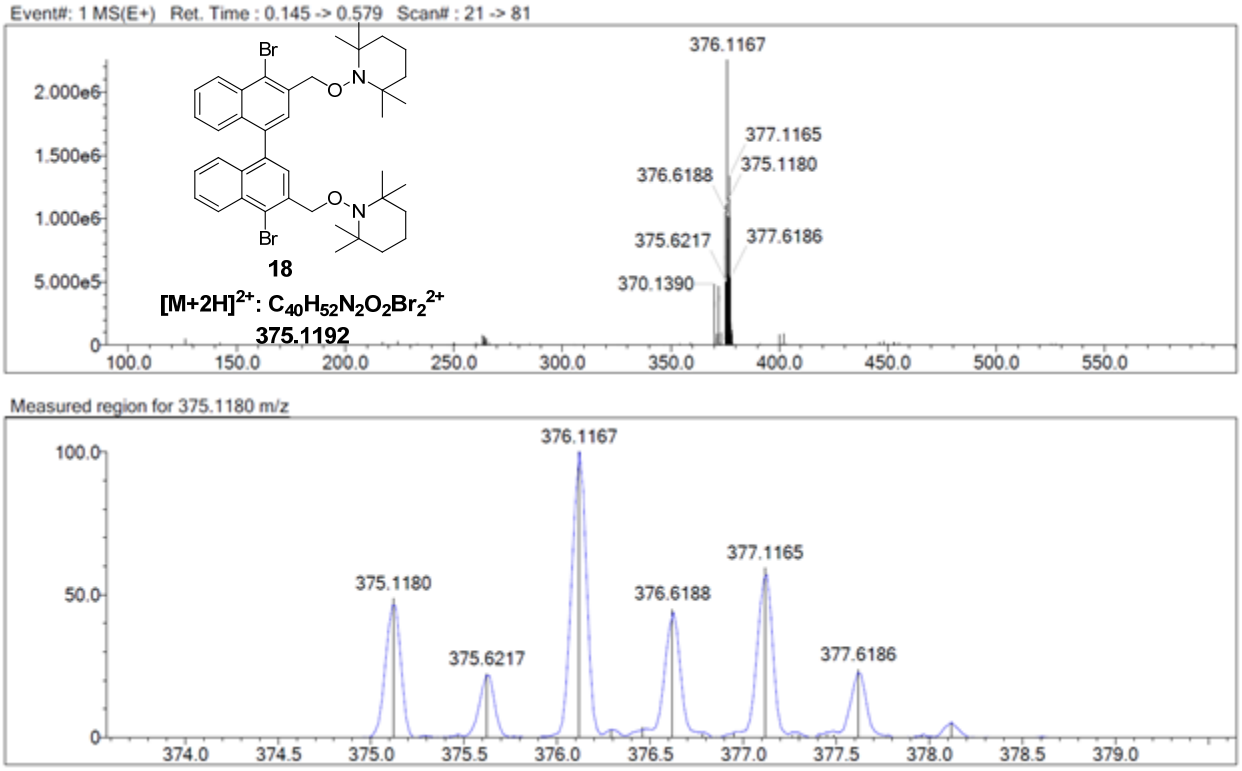

Figure S79. IT–TOF–MS (ESI) of **18.**

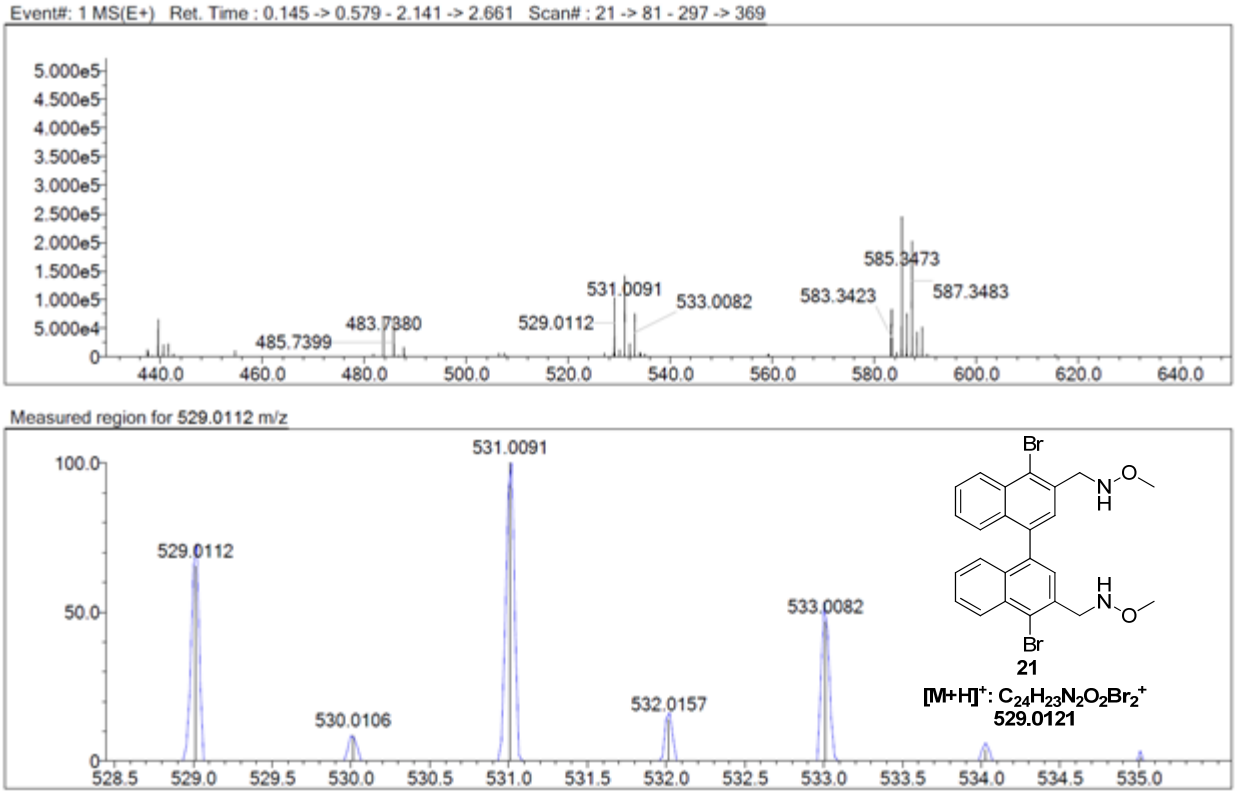

Figure S80. IT–TOF–MS (ESI) of **21.**

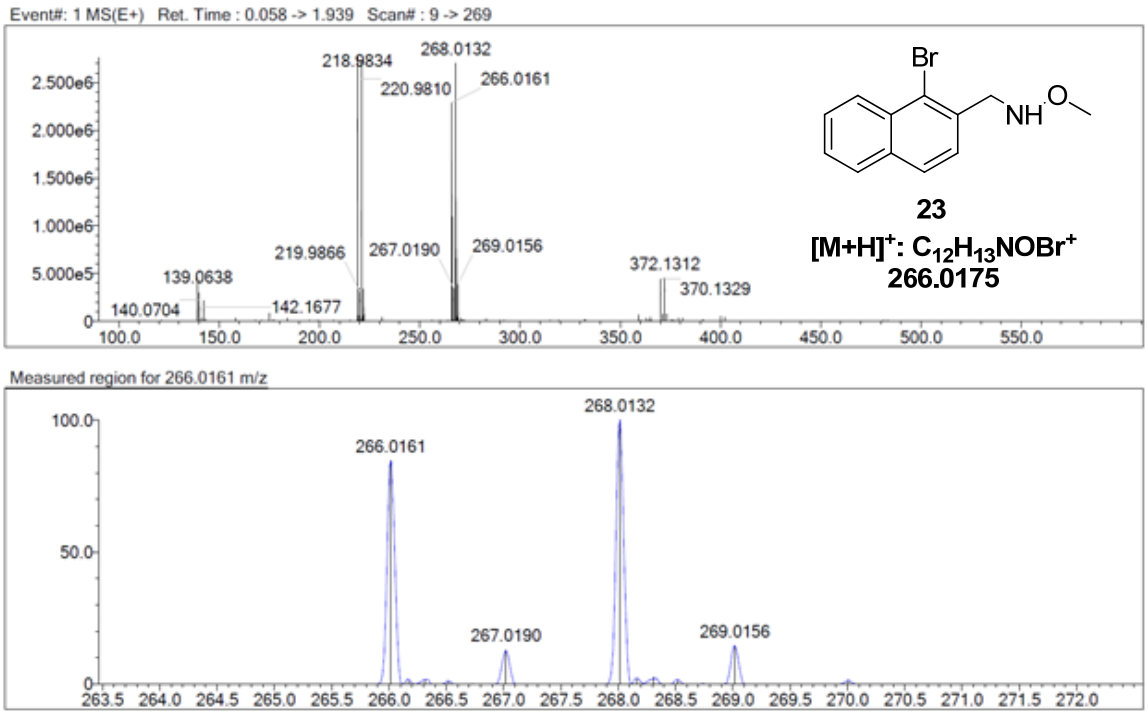

Figure S81. IT–TOF–MS (ESI) of **23.**

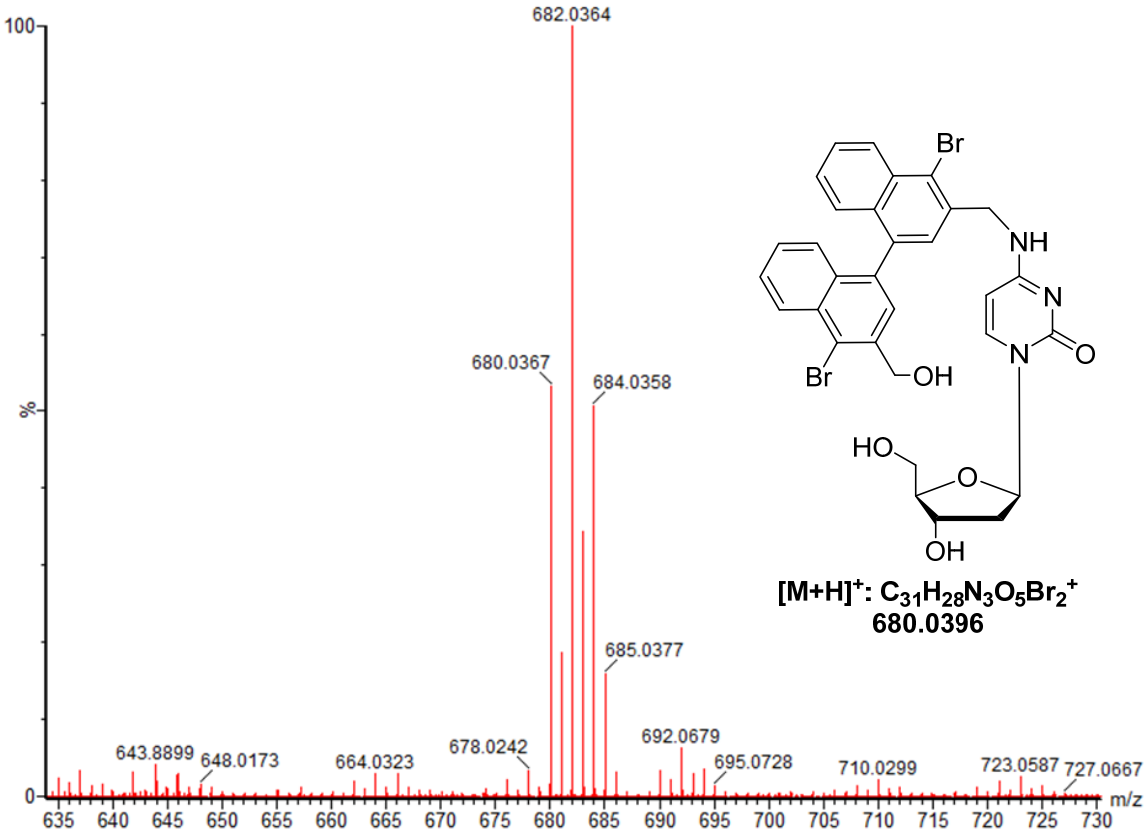

Figure S82. IT–TOF–MS (ESI) of **24.**

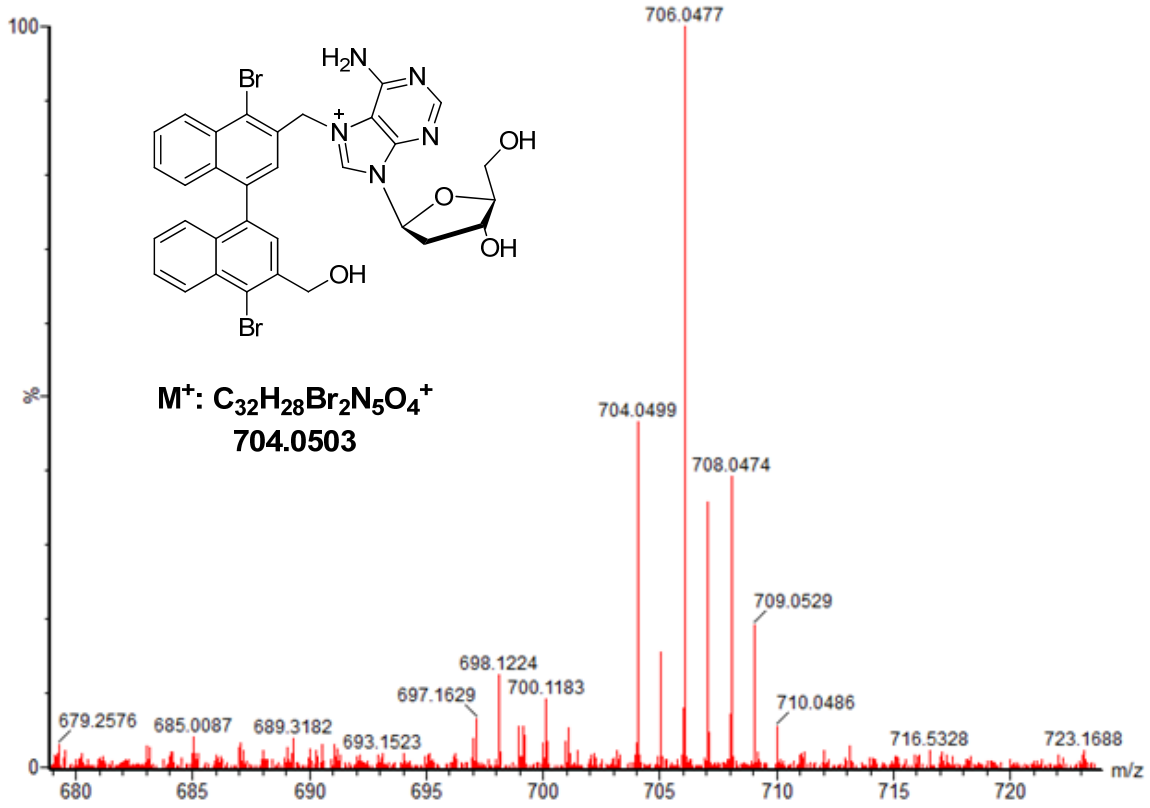

Figure S83. IT–TOF–MS (ESI) of **25a.**

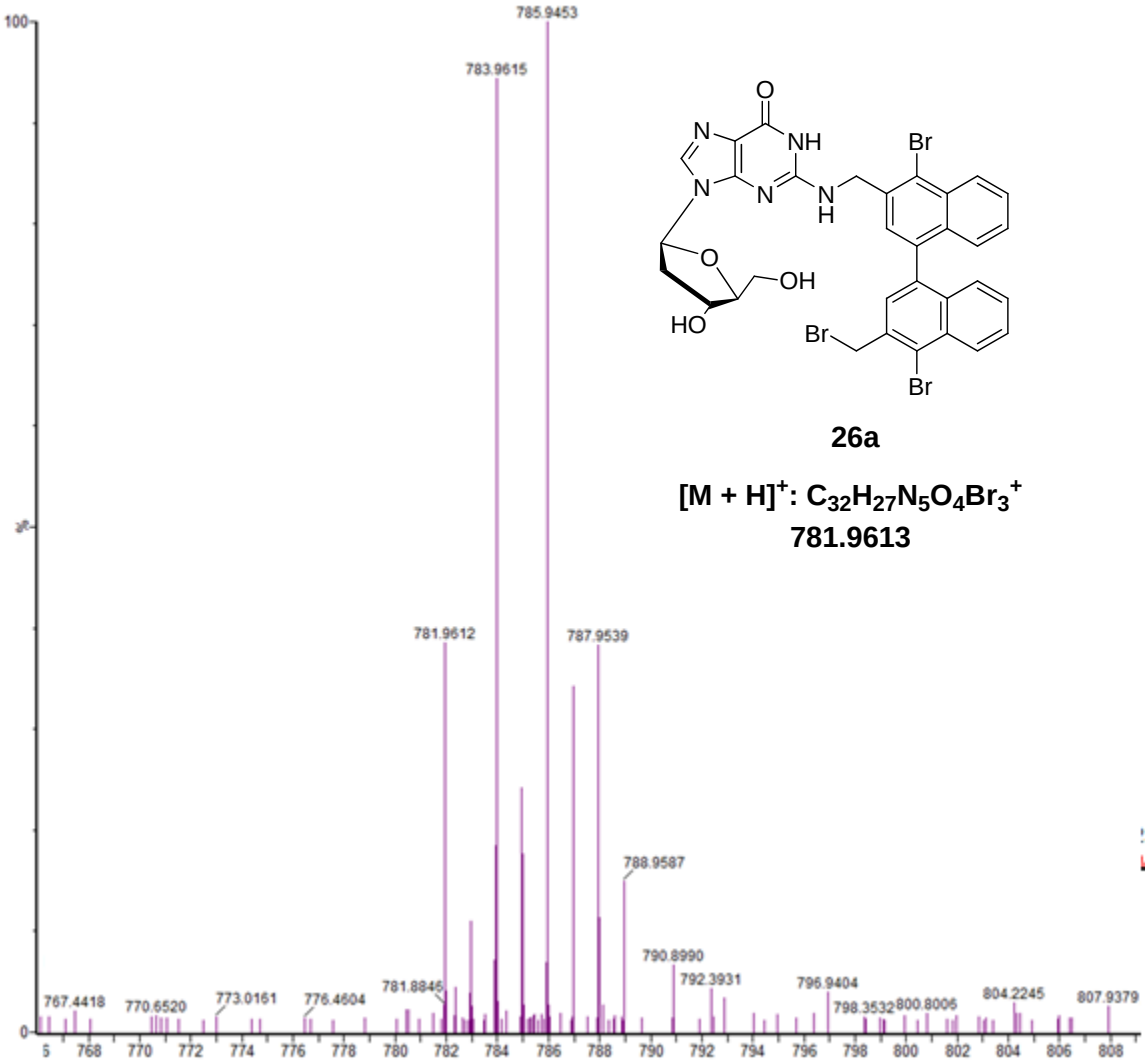

Figure S84. IT–TOF–MS (ESI) of **26a.**

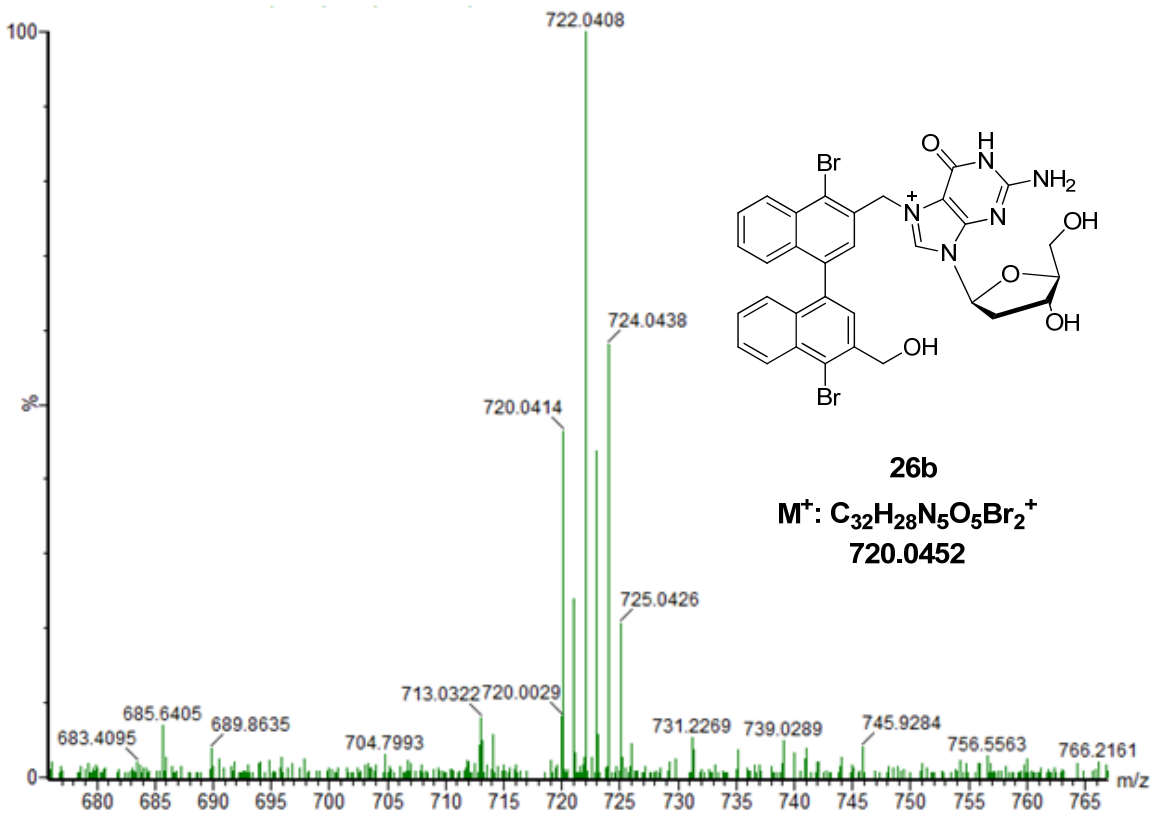

Figure S85. IT–TOF–MS (ESI) of **26b.**

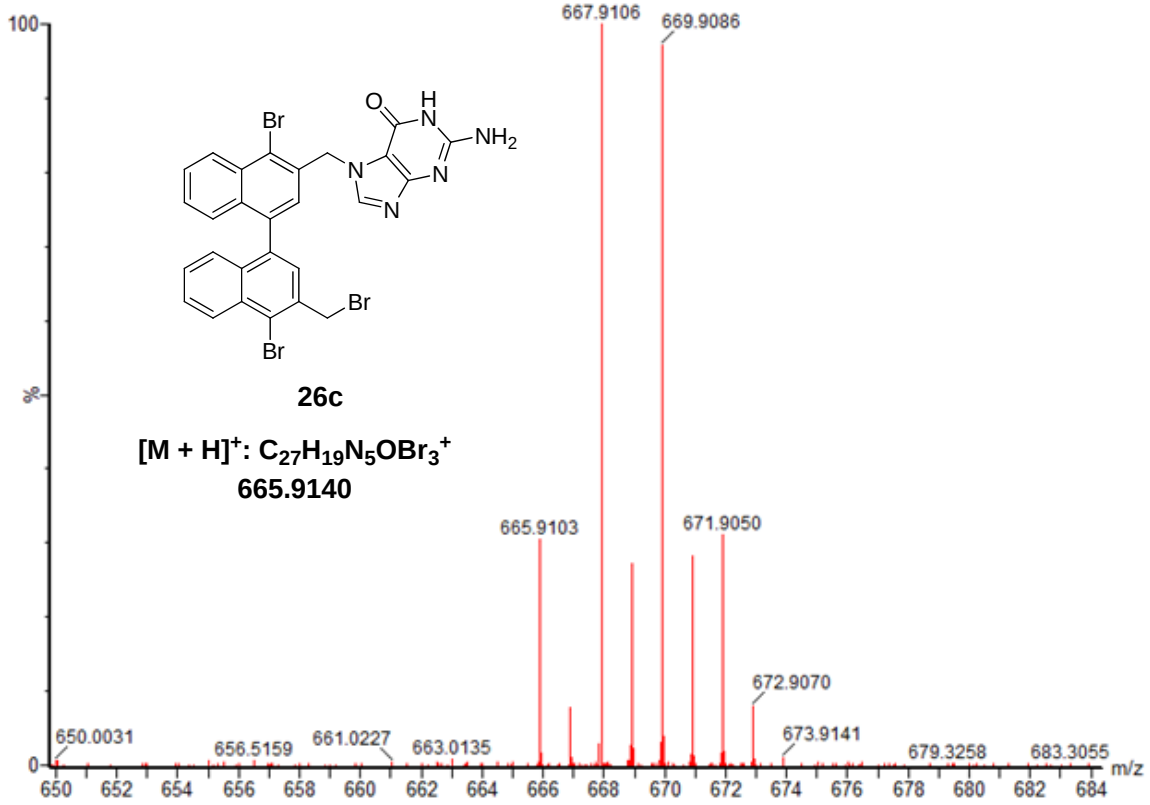

Figure S86. IT–TOF–MS (ESI) of **26c.**

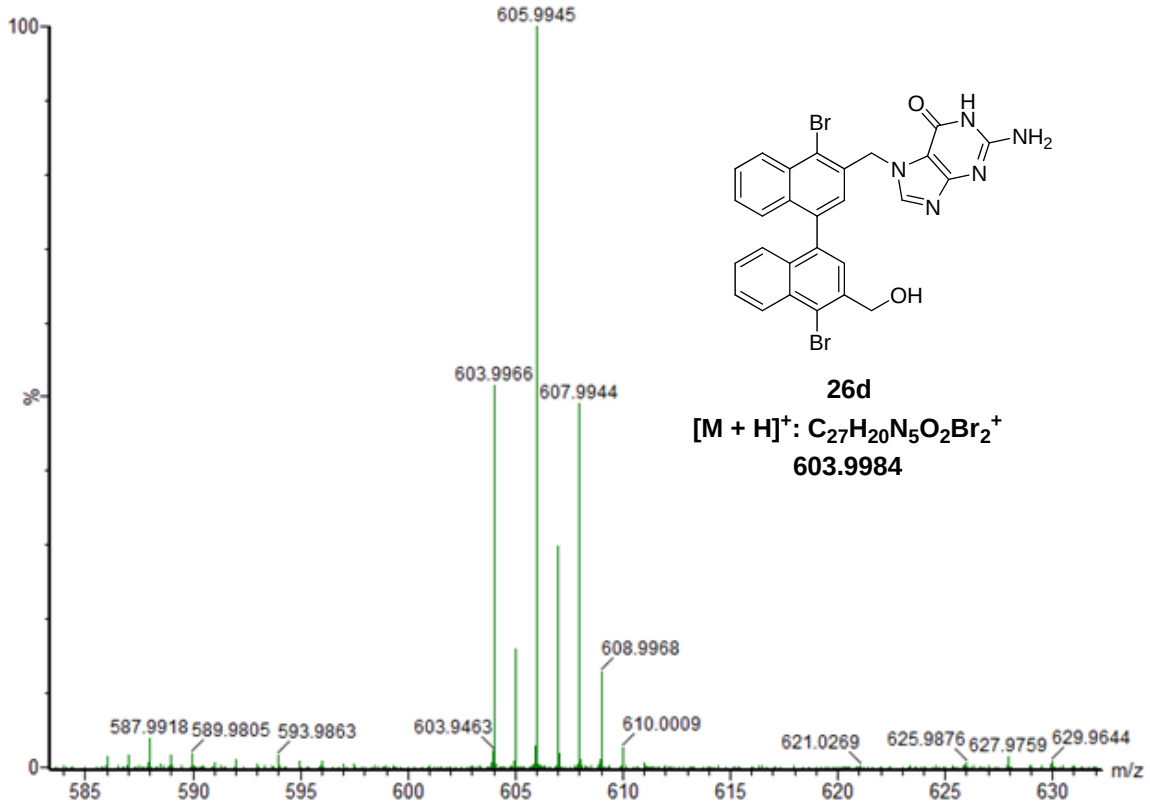

Figure S87. IT–TOF–MS (ESI) of **26d.**